Charge carrier dynamics in colloidal quantum dots: Tracking the dance of electrons and holes by ultrashort laser pulses

Lenngren, Nils

2015

Charge carrier dynamics in colloidal quantum dots

Tracking the dance of electrons and holes by ultrashort laser pulses

Nils Lenngren

Lund University

DOCTORAL DISSERTATION
by due permission of the Faculty of Science, Lund University, Sweden.

To be defended at lecture hall B, Center for Chemistry and Chemical Engineering, Getingevägen 60, Lund, Friday 6 November 2015, 10:15.

Faculty opponent
Gregory D. Scholes
Department of Chemistry
Princeton University

Organization	Document name
LUND UNIVERSITY Chemical Physics Department of Chemistry P.O. Box 124 SE-221 00 LUND, Sweden	Doctoral dissertation
Author(s)	Date of issue 2015-10-13
Nils Lenngren	Sponsoring organization

Title and subtitle

Charge carrier dynamics in colloidal quantum dots: Tracking the dance of electrons and holes by ultrashort laser pulses

Abstract

Quantum dots (QDs) are semiconductor nanocrystals with quantum confinement. This thesis uses various time-resolved spectroscopic techniques to study ultrafast charge carrier dynamics in colloidal CdSe quantum dots that are important both from a theoretical point of view and for their relevance for solar cell applications. Using 2D electronic spectroscopy, we follow charge carrier relaxation and trapping, demonstrating the power and relevance of this technique to QDs. The 2D spectroscopy and other ultrafast techniques allow us to distinguish between trap states with different characteristics with respect to energy level, lifetime and localization. We characterize energy transfer in films of QDs of different sizes, using ultrafast experiments and a detailed theoretical description of the film and QD geometry. Electron and hole transfer is affected by trapping, by the shell in core–shell structures, and by charging of the QD during injection of several excited electrons. Finally, we study the formation and decay of multiple excitons in QDs. Together, the techniques reveal a rich picture of processes and show how these can be controlled for more efficient solar cells.

Key words: Quantum dots, ultrafast spectroscopy, CdSe, charge carrier dynamics

Classification system and/or index terms (if any)

Supplementary bibliographical information	Language English
ISSN and key title	ISBN 978-91-7422-411-5 (print) 978-91-7422-413-9 (PDF)
Recipient's notes	Number of pages: 204 / Price
	Security classification

Signature _____ Date _____

Charge carrier dynamics in colloidal quantum dots

Tracking the dance of electrons and holes by ultrashort laser pulses

Nils Lenngren

PhD Thesis
2015

Lund University

Charge carrier dynamics in colloidal quantum dots: Tracking the dance of electrons and holes by ultrashort laser pulses

Printed in Sweden by Media-Tryck, Lund, 2015

Chemical Physics
Department of Chemistry
Lund University
P.O. Box 124
SE–221 00 Lund
Sweden

http://www.chemphys.lu.se

ISBN 978-91-7422-411-5

To P.-O. Fogelberg

Abstract

Quantum dots (QDs) are semiconductor nanocrystals with quantum confinement. This thesis uses various time-resolved spectroscopic techniques to study ultrafast charge carrier dynamics in colloidal CdSe quantum dots that are important both from a theoretical point of view and for their relevance for solar cell applications. Using 2D electronic spectroscopy, we follow charge carrier relaxation and trapping, demonstrating the power and relevance of this technique to QDs. The 2D spectroscopy and other ultrafast techniques allow us to distinguish between trap states with different characteristics with respect to energy level, lifetime and localization. We characterize energy transfer in films of QDs of different sizes, using ultrafast experiments and a detailed theoretical description of the film and QD geometry. Electron and hole transfer is affected by trapping, by the shell in core–shell structures, and by charging of the QD during injection of several excited electrons. Finally, we study the formation and decay of multiple excitons in QDs. Together, the techniques reveal a rich picture of processes and show how these can be controlled for more efficient solar cells.

Populärvetenskaplig sammanfattning

Vad händer när en halvledarkristall blir väldigt liten? Ett halvledarmaterials optiska och elektriska egenskaper hänger ihop med hur partiklarna som bär elektrisk laddning, elektroner och hål, uppför sig. (En elektron är en negativt laddad partikel. Ett hål kan beskrivas som en positivt laddad bubbla i ett hav av elektroner, och precis som med bubblor är det ibland enklare att titta på hålen än på allt runtomkring dem.) En tillräckligt stor halvledarkristall är praktiskt taget oändligt stor för laddningsbärarna, men när kristallen blir så liten att den hindrar laddningsbärarnas rörelse påverkas också deras beteende, som om de har drabbats av klaustrofobi. Till exempel förändras halvledarens förmåga att ta upp, absorbera, ljus beroende på kristallens storlek. Detta fenomen kan beskrivas med hjälp av kvantmekanik, och kristaller som är små nog att stänga in laddningsbärare kallas därför kvantprickar.

Ett välundersökt material för kvantprickar är kadmiumselenid. Kvantprickar av kadmiumselenid är några nanometer (nano- betyder miljarddels) stora, och består av hundratals till tusentals atomer. De är bland annat lätta att framställa uppslammade i lösning, så kallade kolloidala kvantprickar. Det går också att ha ett annat material, till exempel zinksulfid, som ett skal runt kadmiumseleniden, vilket ger en så kallad kärn–skalkvantprick. För att kvantprickarna ska vara lösliga i olika lösningsmedel eller gå att fästa på ett underlag täcks de med molekyler, så kallade täckmedel, till exempel fettsyran oljesyra.

Solceller är ofta gjorda av halvledare som absorberar ljus, och därför är det lätt att fråga sig om kvantprickar kan vara användbara i solceller, eftersom man kan styra hur de absorberar ljus. Det visar sig också att kvantprickar har flera andra egenskaper som kan göra solceller effektivare. I den här avhandlingen har vi studerat några sådana egenskaper och hur de påverkar processer i kvantprickar.

Många intressanta processer i kvantprickar sker väldigt

snabbt, på en tidsskala från nanosekunder till femtosekunder (miljondels nanosekunder). För att kunna studera dem har vi därför använt korta laserpulser, som gör att vi kan följa vad som händer efter att kvantprickarna absorberat ljus. Vi kan till exempel följa deras absorptionsförmåga (transient absorption) eller hur de sänder ut ljus igen (tidsupplöst fluorescens). En särskilt avancerad metod som vi har använt är 2D-spektroskopi, som kallas så för att den ger hög upplösning i två dimensioner, både vilken ljusenergi som kvantpricken tar upp från början och vilka olika energier som den sedan absorberar.

När kvantprickar tar upp ljus kan en elektron ta upp energin i ljuset och lämna ett hål efter sig. Tillsammans kallas elektron–hålparet en exciton. Likt en nyuppblåst såpbubbla ändrar excitonen på sig, relaxerar, tills den hittat sin lägsta energi, som den sedan behåller tills såpbubblan spricker eller elektronen och hålet återförenas. Vi har följt relaxeringen med 2D-spektroskopi och sett detaljer som inte tidigare har kunnat ses.

Medan de relaxerar kan elektronen och hålet i en exciton fastna i så kallade fällor, som är tillstånd som de sedan har svårt att komma loss ifrån. Fällor uppstår vid oregelbundenheter i kristallen, till exempel vid täckmedelsmolekylerna på ytan. Vi har tittat på olika sorters fällor med både 2D-spektroskopi och andra metoder.

För att kvantprickar ska kunna användas i solceller måste elektronen och hålet skiljas åt, genom att en av dem överförs till ett annat material, injiceras. Det kan också vara praktiskt att överföra hela excitonen från kvantprick till kvantprick. Vi har följt dessa överföringsprocesser och hur de påverkas av kvantprickarnas egenskaper och andra processer.

En egenskap hos kvantprickar som kan vara nyttig i solceller är deras förmåga att under vissa omständigheter omvandla en absorberad foton (ljuspartikel) till två eller fler excitoner. För att lära oss mer om denna process har vi imiterat den genom att belysa kvantprickarna med så starkt ljus att en kvantprick kan hinna absorbera flera fotoner från en laserpuls. Sedan har vi följt vad som händer med excitonerna när de relaxerar eller när en elektron injiceras.

Sammantaget visar det sig att kvantprickar har många egenskaper som är intressanta i sig, men också är möjliga att styra för att förbättra deras användbarhet i solceller. Förhoppningsvis kan detta leda till billiga och effektiva solceller som bidrar till att lösa världens energiproblem.

List of Publications

This thesis is based on the following papers, which will be referred to by their Roman numerals in the text. Paper II–VI were reprinted with permission from the journals listed here. Copyright 2012–2014 American Chemical Society.

I **Exciton relaxation and trapping in thiol-capped CdSe quantum dots studied by 2D electronic spectroscopy**
N. Lenngren, M.A. Abdellah, K. Zheng, D. Zigmantas, K. Žídek, T. Pullerits.
Manuscript to be submitted to Nano Letters.

II **Ultra long-lived radiative trap states in CdSe quantum dots**
M. Abdellah, K.J. Karki, N. Lenngren, K. Zheng, T. Pascher, A. Yartsev, T. Pullerits.
J. Phys. Chem. C, ***2014***, *118 (37), pp 21682–21686*.

III **Ultrafast charge transfer from CdSe quantum dots to p-type NiO: Hole injection vs hole trapping**
K. Zheng, K. Žídek, M. Abdellah, W. Zhang, P. Chábera, N. Lenngren, A. Yartsev, T. Pullerits.
J. Phys. Chem. C, ***2014***, *118 (32), pp 18462–18471*.

IV **Directed energy transfer in films of CdSe quantum dots: Beyond the point dipole approximation**
K. Zheng, K. Žídek, M. Abdellah, N. Zhu, P. Chábera, N. Lenngren, Q. Chi, T. Pullerits.
J. Am. Chem. Soc., ***2014***, *136 (17), pp 6259–6268*.

V **Ultrafast dynamics of multiple exciton harvesting in the CdSe–ZnO system: Electron injection versus Auger recombination**
K. Žídek, K. Zheng, M. Abdellah, N. Lenngren, P. Chábera, T. Pullerits.
Nano Lett., ***2012***, *12 (12), pp 6393–6399*.

VI **Multiexciton absorption cross sections of CdSe quantum dots determined by ultrafast spectroscopy**
N. Lenngren, T. Garting, K. Zheng, M. Abdellah, N. Lascoux, F. Ma, A. Yartsev, K. Žídek, T. Pullerits.
J. Phys. Chem. Lett., ***2013***, *4 (19), pp 3330–3336*.

Contribution Report

I **Exciton relaxation and trapping in thiol-capped CdSe quantum dots studied by 2D electronic spectroscopy**
I led the planning of the experiments, was responsible for the experiments, took major part in the data analysis and discussions, and wrote the main part of the manuscript.

II **Ultra long-lived radiative trap states in CdSe quantum dots**
I took part in the planning of experiments, participated in preliminary experiments, took part in discussions and contributed to the writing of the paper.

III **Ultrafast charge transfer from CdSe quantum dots to p-type NiO: Hole injection vs hole trapping**
I took part in the experiments and discussions, and contributed to the writing of the paper.

IV **Directed energy transfer in films of CdSe quantum dots: Beyond the point dipole approximation**
I took part in the experiments and discussions, and contributed to the writing of the paper.

V **Ultrafast dynamics of multiple exciton harvesting in the CdSe–ZnO system: Electron injection versus Auger recombination**
I took part in the experiments and discussions, and contributed to the writing of the paper.

VI **Multiexciton absorption cross sections of CdSe quantum dots determined by ultrafast spectroscopy**
I took part in the planning of experiments, was responsible for most spectroscopy experiments, did the data analysis, took major part in discussions and wrote a major part of the paper.

Contents

Papers

Chapter 1

Introduction

1.1 Discovery of quantum dots

In the early 1980s, solid state physicists started to take an interest in what happens when semiconductor crystals become very small, on the order of a few to tens of nanometres. Such crystals were created in several different ways, such as epitaxial growth on the surface of another material, suspended in aqueous solution or as inclusions in a glass.[1–3]

The electrons in semiconductors populate electronic states in a band of allowed energies. The intrinsic semiconductors feature a fully populated *valence band*, followed by a *band gap* without states and an unpopulated *conduction band*. The longest-wavelength (lowest-energy) light that a macroscopic semiconductor can absorb is determined by the band gap, which is a material constant.[4] In bulk semiconductors, changing the band gap means changing the material. However, it was found that the absorption spectra, and thus the colour, of the semiconductors change with crystal size when the crystals are small enough. This was called the *quantum size effect*.[1–3] Semiconductor nanocrystals displaying the quantum size effect were first called "quantum dots" (QDs) in 1986, in that case describing nanocrystals embedded in nanowires.[5]

From the perspective of quantum mechanics, the quantum size effect is in itself not that surprising. It is a feature already of the most simple quantum mechanical model, the *particle in a box* or *infinite square well*.[6] In this model, a particle of mass m is confined along a stretch of length a, the box (or square well). Inside the box, the potential is 0; outside, it is infinite. The energy E of the particle is given by the time-independent Schrödinger equation, which inside the box takes the form:

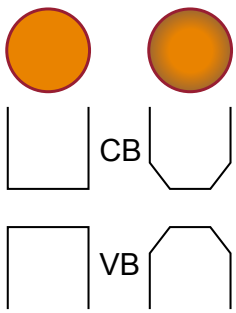

Figure 1.1. *Schematic of a core (left) and gradient core–shell (right) QD, along with sketches of their conduction band (CB) and valence band (VB) potentials.*

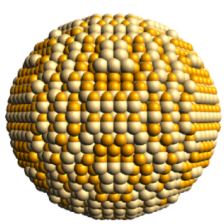

Figure 1.2. *Crystal structure of a quantum dot without capping agent. Picture courtesy of Thorsten Hansen.*

$$-\frac{\hbar^2}{2m}\frac{\mathrm{d}^2\psi(x)}{\mathrm{d}x^2} = E\psi(x) \tag{1.1}$$

where $\hbar$ is Planck's reduced constant ($1.05 \cdot 10^{-34}$ J·s)[7] and $\psi(x)$ is the time-independent wave function. The solutions to this differential equation are a set of energies E_n:

$$E_n = \frac{n^2\pi^2\hbar^2}{2ma^2} \tag{1.2}$$

where n is any positive integer.[6] The energy difference ΔE between two adjacent levels n and $n-1$ is

$$\Delta E = \frac{(2n-1)\pi^2\hbar^2}{2ma^2}. \tag{1.3}$$

An electron excited by light in a quantum dot can be modelled as a particle in a box, where the box is determined by the boundaries of the dot (see Figure 1.1). We see that the change in energy of a given excitation ΔE increases as a decreases. An electron will need more energy to be excited, meaning that absorption will shift towards the blue. Furthermore, the particle-in-a-box model shows that in QDs, only certain discrete energies are allowed. Conversely, if a is large enough, essentially any energy is possible.

Of course, this is only a very rough sketch of the electronic structure of QDs. A full description uses more realistic shapes of the band potentials, considers what happens in the valence band after an electron is removed, and defines when the nanocrystal is small enough to be a quantum dot. We return to the quantum mechanical modelling of QDs in Chapter 3 and Chapter 6.

1.2 Development of quantum dots and scope of the thesis

As mentioned previously, quantum dots have been produced by several different methods since the beginning of the field. The work presented in this thesis is on colloidal QDs, i.e. where the QDs are synthesised as colloids with a cover of capping agents, suspended in a solution. The capping agents are organic molecules that bind to the QD surface. They improve the solubility in polar or nonpolar solvents, passivate dangling orbitals on the nanocrystal surface, and can enable chemical interactions with other nanostructures.[8] In some of the work described in this thesis, the QDs are deposited on a surface or included in a solvent glass, but the capping agents remain.

A prerequisite for the investigation of QD properties and their use in applications has been the development of reliable

synthetic techniques. Regarding colloidal quantum dots, an important target has been a narrow size distribution without further purification steps.[9] Another line of pursuit has been the development of so-called core–shell quantum dots. Early in the exploration of QDs, it was recognized that covering a QD (the core) with a different semiconductor material (the shell) in core–shell structures would be advantageous.[10] Originally, core–shell QDs were synthesized by first synthesizing the cores, then adding the precursors of the shell material.[11] More recently, a single-step method that creates a gradient from core to shell was developed,[12] which was used here (see Figure 1.1). We will return to it in Chapter 2.

Although quantum dots have been made from many different semiconductor materials, this thesis will be exclusively about CdSe quantum dots. CdSe is a well-characterized model or "toy" material for QDs, due to some of its advantageous properties. For example, it is easy to synthesize CdSe QDs with high quality.[4]

When we discuss core–shell QDs, the shell material is always ZnS (denoted as (CdSe)ZnS quantum dots), which means that the band alignment is of type I. In type I core–shell QDs, the valence band is higher in energy in the core than in the shell, and vice versa for the conduction band. As a result, both electrons and holes have the lowest potential in the core, giving high confinement and chemical stability.[13]

A disadvantage of CdSe is the toxicity of cadmium.[14] One could think of several ways of dealing with this issue. One would be to develop systems, on both a chemical and a societal level, that ensure that the QDs are shielded from contact with the environment. Examples of chemical systems would be shell materials and specific capping agents.[15] Another would be to use the understanding gained from CdSe to construct similar systems from materials that are more friendly to the environment but less friendly to the brain of the researcher. Two such materials are $CuInS_2$ (copper indium sulphide) and CZTS (copper zinc tin sulphide).[16–18]

1.3 Dye-sensitized solar cells and quantum dot-sensitized solar cells

As awareness has increased of the consequences of CO_2 emission to the atmosphere and the possibility of decreased fossil fuel production (peak oil), alternative energy sources have received more attention. The most fundamental and in theory the most promising such source is the sun. Indeed, sunlight provides the Earth with more than 10,000 times the energy consumed by humanity. If this energy can be collected and turned into electricity or fuels with an efficiency of 10%, covering 0.1% of

the surface area of the Earth with solar power plants would be enough to provide all the energy needed.[19]

For many years, research into generating electricity from sunlight, i.e. photovoltaics, was focused on solar cells based on silicon. This has changed during the last 25 years, starting with the development of the dye-sensitized solar cell (DSSC).[19] The first practical DSSC was described in 1991.[20] In this type of solar cell, light is absorbed by dye molecules that are attached to a metal oxide (often TiO_2) in nanoparticle form to provide the largest possible surface area. The excited electrons in the dyes are transferred to the metal oxide, which is connected to an electrical circuit. The circuit is completed by an electrolyte with a redox pair such as I^-/I_3^-. Compared to previous solar cells, the dye-sensitized solar cell require much less pure materials, leading to lower cost.[21]

Considering the high extinction coefficient and tunable band gap of QDs, it is not surprising that QDs were suggested as sensitizers at the same time as DSSCs entered the solar cell field, in the so-called quantum dot-sensitized solar cell (QDSSC).[21] However, it is only within the last few years that QDSSCs have truly started to show their potential, with the highest reported efficiency of QDSSCs and related QD-based solar cell systems going from 3% in 2010 to 9.9% in 2015. Despite this rapid increase, the efficiency is still quite low compared to competing technologies (see Figure 1.3).[22]

In addition to their extinction coefficient and band gap,[23,24] QDs have a number of other properties that are of interest for solar cell applications, such as multiple exciton generation (MEG, see Chapter 6),[25–29] hot electron transfer,[21] and high stability[30]. Using multiple exciton generation and hot electron transfer, QDs could potentially break the Shockley–Queisser thermodynamic limit, which arises from a consideration of the solar spectrum and the properties of a single-junction solar cell. Photons with energies smaller than the band gap will not be absorbed, and photons with energies larger than the band gap will lose the excess energy as heat. The theoretical maximum efficiency of a solar cell made from one semiconductor material is thus no more than $\sim$30% for blackbody radiation,[31] increasing to 31–33% if the absorption of the atmosphere is taken into account[32]. Furthermore, the Shockley–Queisser limit disregards other practical issues that diminish the real efficiency.[33]

This thesis deals with application of QDs in light harvesting in many aspects. The thesis is organized as follows. After this introductory chapter, the fabrication of samples is briefly described in Chapter 2, followed by descriptions of the experimental methods along with short motivations for using them. Our results are described in four chapters organized thematically: charge carrier relaxation (Paper **I**), charge carrier trapping (Paper **I**, **II**,

and **III**), energy and charge transfer (Paper **III**, **IV**, and **V**), and multiexcitons (Paper **V** and **VI**). Some of the papers upon which the thesis is based deal with two themes, and will therefore be described in two chapters. Some concluding remarks are given in the final chapter. The aim of the thesis is, rather than achieving a record-efficiency solar cell, to understand fundamental charge carrier dynamics in the system and obtain knowledge showing the real potential of QD-based photovoltaics.

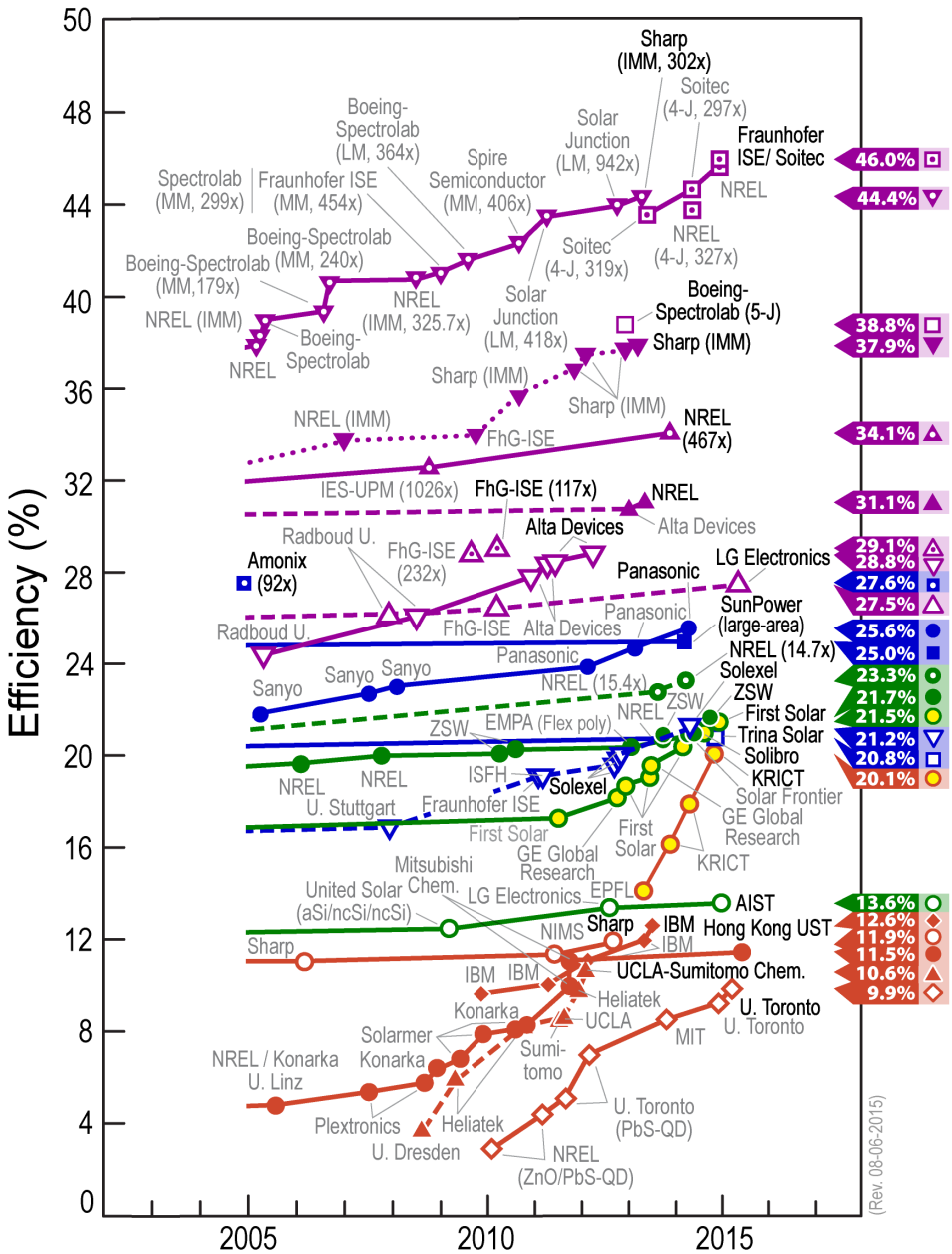

Figure 1.3. *Best research-cell efficiencies of solar cells. Purple: Multijunction cells and single-junction GaAs. Blue: Crystalline Si. Green: Thin-film cells. Orange: Emerging technologies, among them perovskite cells (circles filled with yellow), dye-sensitized cells (circles filled with white) and quantum dot cells (diamonds filled with white). Adapted from*[22]*, courtesy of the National Renewable Energy Laboratory, Golden, Colorado.*

Chapter 2

Materials and methods

Quantum dots were synthesized using a wet chemical method, and then put into various kinds of samples. The samples were studied using mainly transient absorption and 2D electronic spectroscopy, as well as time-resolved photoluminescence.

2.1 Synthesis of quantum dots

2.1.1 Core quantum dots

Most core QDs used in this thesis were synthesized at the department, the exception being the 5 nm QDs used in the multiexciton cross section measurements (Paper **VI**) which were purchased dispersed in toluene from Sigma-Aldrich (Lumidot) and diluted.

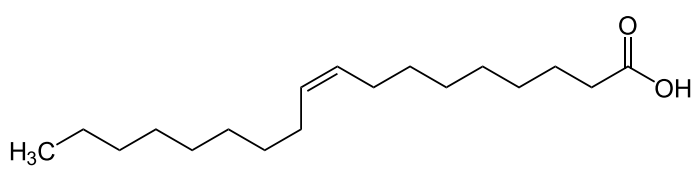

Figure 2.1. *Structural formula of oleic acid.*

In the synthesis used at the department,[24,34] the cation precursor is created by heating CdO with oleic acid in 1-octadecene solution. Oleic acid (OA, see Figure 2.1) will also form the capping agent of the QDs. The temperature is then increased to the desired reaction temperature (180–320 °C), and the anion precursor, Se in trioctylphosphine, is injected, which starts the growth

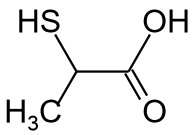

Figure 2.2. *Structural formula of 2-MPA.*

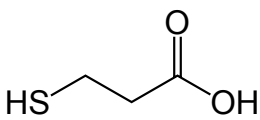

Figure 2.3. *Structural formula of 3-MPA.*

of the QDs. The growth is stopped after seconds to minutes by quickly immersing the reaction vessel in an ice bath. By changing the reaction temperature or growth time, the final size of the QDs can be adjusted. After the synthesis, the QDs were purified twice and transferred to hexane or toluene solution.

2.1.2 Core–shell quantum dots

Gradient core–shell quantum dots were synthesized at the department.[29,35] The synthesis of gradient core–shell QDs[12,36] takes advantage of the different crystal growth rates of core and shell materials. Both core and shell precursors are present in the reaction mixture. When the reaction is started, the core material grows fastest, meaning that crystals will be almost pure core material, but as the core precursors are depleted, the outer layers of the QDs will be almost pure shell material, with a gradient in-between.

As with core QDs, the size, in this case including the shell thickness, is determined by changing the reaction temperature and time (300–325 °C, 5 s–5 min). The procedure is also similar to the synthesis of core QDs in other respects, but the cation precursor contains both CdO and ZnO, and the anion precursor contains both Se and S.

2.1.3 Functionalization

QDs that are used for sensitization need to have the oleic acid replaced by a bifunctional capping agent, i.e. a capping agent with two functional groups—one interacting with the nanocrystal surface and one interacting with the surface of the sensitized material. Two bifunctional capping agents were used in this work, namely 2-mercaptopropionic acid (2-MPA) and 3-mercaptopropionic acid (3-MPA, see Figure 2.2 and 2.3). In Paper **I**, **III** and **IV**, 3-MPA was used; in Paper **V**, 2-MPA. Both molecules contain a thiol group, which reacts with the QD surface, and a carboxylic acid group. The carboxylic acid groups, apart from attaching to other surfaces, also make the QDs soluble in polar solvents rather than nonpolar as in the case of OA. For this reason, the QDs are resuspended in ethanol after replacement of the capping agents.

2.2 Sample preparation

In the samples studied in this thesis, QDs have been placed in a number of different environments, namely colloidal suspension in a solvent, in a solvent glass, deposited on an acceptor of electrons or holes, or deposited on a glass surface.

Solvents used were hexane or toluene (for oleic acid-capped QDs) and ethanol (for MPA-capped QDs). The band-edge transition optical density was kept under 0.3 in 0.5 or 1 mm cuvettes.

In Paper **I**, the QDs were measured in a solvent glass. The material for a solvent glass needs to be a good solvent for the solute at all temperatures between room temperature and the measurement temperature, but should not crystallize in the solid state. This is usually accomplished by mixing different solvents with similar properties that do not crystallize well together. In this work, the QDs were suspended in a 1:1 mixture of methanol and ethanol, which forms a decent solvent glass at 77 K.

MPA-capped QDs were attached to mesoporous NiO films (Paper **III**) or ZnO nanoparticle films (Paper **V**) by coating the films in QD suspension and incubating in the dark.

QDs were spin-coated onto a silica glass surface for two reasons: to study energy transfer between different sizes of QDs (Paper **IV**) and to check the effects of QD attachment to a surface and charge transfer separately (Paper **V**). The energy levels of the glass are such that no charge transfer can take place. This was used to verify that surface trapping or agglomeration do not cause fast decays that could be mistaken for charge transfer.

2.3 Measurement techniques

2.3.1 Steady-state techniques

Steady-state absorption spectroscopy is one of the most fundamental spectroscopy techniques, describing how the light intensity I with a given frequency ν changes as it goes through a sample:

$$\lg \frac{I_0}{I} = A(\nu) = \epsilon(\nu) l c, \tag{2.1}$$

where A is defined as the absorbance, ϵ is the extinction coefficient of the absorbing species, l is the path length through the sample and c is the concentration of the absorbing species. An important parameter in the description of QD absorption spectra is the position of the first (band-edge) absorption peak, from which the size of the QDs can be determined.[37]

Steady-state absorption spectra were measured in a UV–vis absorption spectrometer (Agilent 845x). Absorption spectra of samples at 77 K were measured in another UV–vis spectrometer (PerkinElmer Lambda 1050), with the samples kept in the cryostat.

Photoluminescence (PL) is the emission of light by a species as it decays from an excited state. Steady-state photoluminescence spectroscopy is also a comparatively simple way of characterizing QDs. We used it to check for energy transfer between QDs (in

Paper **IV**) and to check the sample quality, e.g. the presence of traps.

Steady-state photoluminescence spectra of QD films and colloidal solutions were measured in a fluorescence spectrometer (Spex 1681), usually with excitation at 470 nm. In the ordered multilayer film study (Paper **IV**), the samples were excited at 420 nm in an N_2 atmosphere.

2.3.2 Transient absorption

Transient absorption spectroscopy (TA) is the extension of absorption spectroscopy to the time dimension. A process is started in the sample by an ultrafast laser pulse (the pump), and the absorbance of another pulse (the probe) after a time delay is measured. By repeating the measurement with different time delays and subtracting the absorbance without pump, a transient absorption trace is obtained.

The typical transient absorption setup used in this work was described in[24] and is shown in Figure 2.4. A femtosecond oscillator (Tsunami) feeds a regenerative amplifier (Spitfire XP, both Spectra Physics) to generate 80 fs laser pulses at 800 nm wavelength and 1 kHz repetition rate. These pulses are converted to pump pulses at 430–470 nm by an optical parametric amplifier (Topas C, Light Conversion) and to probe pulses (a broad supercontinuum spectrum) by a sapphire plate. Part of the probe beam is split off as a reference; both beams are dispersed in a spectrograph and detected by a diode array (Pascher Instruments). In Paper **VI**, narrow-band probe pulses were used instead of a supercontinuum. These are generated in a nonlinear optical parametric amplifier (NOPA) and detected by photodetectors.

For Paper **II**, a femtosecond pump–nanosecond probe setup with two synchronized lasers was used. Pulses from an amplified laser (CPA 2001, 1 kHz repetition rate) were sent into a 1 mm thick BBO crystal to generate the second harmonic at 387 nm, which was used as the pump beam[28]. The intensity of the pump beam was controlled by a compensator–analyzer combination. A pulsed Nd:YAG diode-pumped laser generated the probe beam at 532 nm. The time delay of the probe beam relative to the pump beam was created by a delay generator triggered by the transistor–transistor logic signal from the amplified laser.

Thin-film samples were kept in N_2 atmosphere during the measurements to avoid QD oxidation.[38]

2.3.3 2D electronic spectroscopy

The result of two-dimensional electronic spectroscopy (2DES) measurements is a series of spectra for a number of *population times*, with *rephasing* and *non-rephasing* spectra at each time as

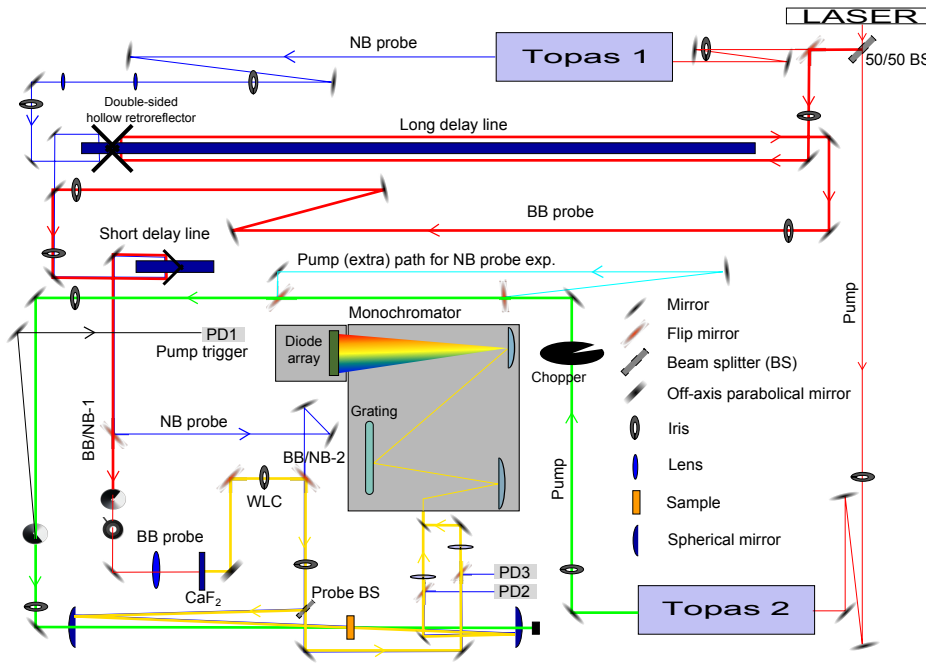

Figure 2.4. *Transient absorption setup used in this work. The setup can be used in broadband (BB) or narrow-band (NB) probe mode. In broadband mode, the signal is detected by the diode array; in narrow-band mode, by the photodetectors PD2 and PD3. Figure courtesy of Pavel Chábera.*

a function of two angular frequency axes ω_1 and ω_3. (As the axes are the result of Fourier transforms, the instrumental output is often given as angular frequency ω, which is converted to energy by multiplication with Planck's reduced constant $\hbar$.) There is a lot of information available, but it is also demanding to interpret. However, if we limit ourselves to the sum of the rephasing and non-rephasing spectra and take the real part of the complex values, it can be thought of as the extension of transient absorption to two dimensions: the ω_1 axis is analogous to the pump frequency, and ω_3 is analogous to the probe frequency. In addition, the off-diagonal peaks (cross peaks) of a 2D spectrum show both coherence and population dynamics between the two states involved.[39]

2DES has in recent years shown its utility when it comes to

showing couplings between different energy levels, as well as achieving high time and energy resolution in QDs and other systems.[40,41] This advantage originates from the properties of the Fourier transform, the shorter laser pulses are in time, the broader their spectra. For conventional transient absorption spectroscopy, this forces a compromise between temporal and spectral resolution, but in 2D spectroscopy, this is avoided by using a series of pulses, enabling simultaneous high time and energy resolution. The downside is longer data acquisition times.

Compared to nuclear magnetic resonance (NMR) spectroscopy, where series of radio-frequency pulses have been used for a long time and 2D NMR was developed in the 1970s,[42] 2DES and its closely related counterpart 2D infrared spectroscopy (2DIR) are rather recent developments. The fundamental theory was developed by Mukamel and co-workers in the beginning of the 1990s,[43,44] and the first successful 2DES experiments were not published until 1998[45]. Since then, the use of 2DES has spread to many different fields.

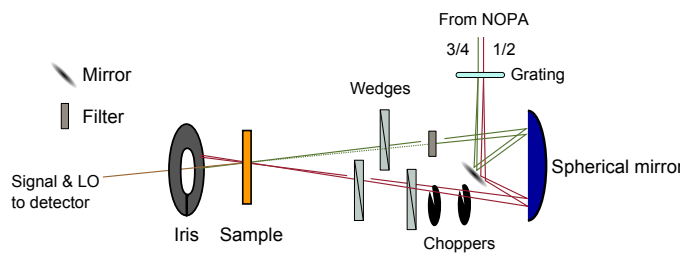

Figure 2.5. *Simplified schematic side view of the core of the 2D setup (after[46]). Pulse 3/4 is delayed relative to pulse 1/2 by a delay line (not shown).*

In Paper **I**, we used a previously described 2D spectroscopy setup[46]. By using diffractive optics and well-considered geometry of optical elements, it has high phase stability. 1030 nm pulses are generated in an Yb:KGW laser, and feed a nonlinear optical parametric amplifier (Light Conversion), whose output is then compressed to 9.2 fs long pulses (FWHM) centred at 600 nm. Pulses are delayed using a delay stage (for population time) and glass wedges (for coherence time) and sent through the sample, with the signal beam being detected via heterodyning with a low-intensity pulse in a phase-matching direction. The interferogram is recorded by a CCD coupled to a spectrograph.

2.3.4 Time-resolved photoluminescence

In time-resolved photoluminescence, the sample is again excited with a short pulse, but the photoluminescence instead of the absorbance is measured with time resolution. Since the bleach signal in the transient absorption experiments with QDs is mainly sensitive to the electrons,[47] time-resolved PL was used to follow the dynamics of holes when they are trapped or injected in a metal oxide. Two different time-resolved PL setups were used, one in Paper **II** and one in Paper **III**. In Paper **II**, a time-correlated single-photon counting setup (PicoQuant) was used, with the sample excited at 438 nm by a 400 kHz pulsed diode laser. The wavelengths of interest were selected with long-pass filters and detected by a fast avalanche photodiode (SPAD, Micro Photon Device).

In Paper **III**, the sample was excited by 410 nm pulses from a second-harmonic generator (Photop technologies, Tripler TP-2000B) fed by a titanium:sapphire passively mode-locked femtosecond laser (Spectra-Physics, Tsunami), emitting at 820 nm. The repetition rate was mainly 80 MHz, but lower repetition rates (down to 1.6 MHz) were used to exclude possible photocharging of QDs. A picosecond streak camera (C6860, Hamamatsu, time resolution <1 ps) operating in single-shot mode coupled to a Chromex spectrograph, triggered by the Ti:sapphire laser, detected time-resolved photoluminescence spectra.

Chapter 3

Relaxation

The most fundamental process taking place after a system is excited to a higher state is relaxation back to the ground state. In quantum dots, the relaxation of both electrons and holes before their final recombination is relevant, giving rise to a complex system of pathways.

3.1 The electronic structure of CdSe quantum dots

As we saw in Chapter 1, even the simple particle-in-a-box model gives a basic understanding of the electronic structures of QDs.

A common model that accounts for the atomic-like behaviour of quantum dots is the particle-in-a-sphere effective-mass model. It combines the *particle in a sphere* model, which is essentially particle in a box in three dimensions with spherical symmetry, with the concept of *effective mass* from bulk solid state theory.[3] The use of effective mass originated in the observation that a charge carrier in a crystal behaves almost like a free particle, just with a different mass.[48] By changing a parameter of the particle (its mass), one can describe what is in fact a change in the medium (a crystal filled with atoms instead of a vacuum). In this sense, it is even possible to regard the absence of electrons as a quasiparticle called a hole. The combination of an electron and a hole can also behave as a quasiparticle, called an exciton.[3] We will describe excitons in more details in Chapter 6. In order to fit the concepts of particle in a sphere and effective mass together, the model assumes that within the sphere that approximately corresponds to the QD surface, electrons and holes behave like free particles with bulk effective mass. This way of "cutting out a piece" of the bulk is sometimes called the envelope function approximation.[3]

The end result is a description not unlike the electronic structure of atoms, with n and L quantum numbers, familiar from

atomic physics, giving rise to $1S$, $1P$, $2S$ states and so forth. There are some notable differences, however. For example, QD states, especially hole states, are more degenerate than atomic states. The degeneracies in the valence band are partially lifted by the mixing of the bulk and envelope function momenta as the total angular momentum F which can be either $3/2$ or $1/2$ in the states considered here. For an example of the electronic structure, see Figure 3.1, which also introduces the shorthand exciton labels that will be used in this chapter and Chapter 4.

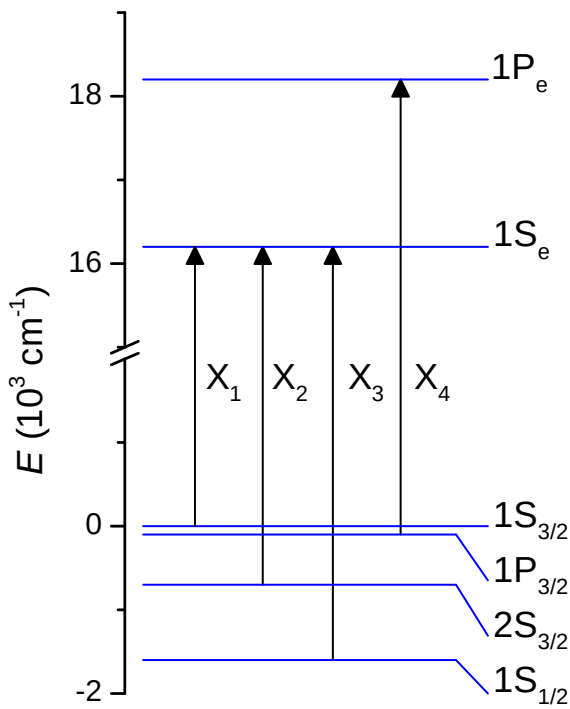

Figure 3.1. *Electron and hole states (blue lines) close to the band edge in a CdSe quantum dot with radius 7.1 nm. The hole states in the valence band are closer together than the electron states in the conduction band and labelled according to total angular momentum. Also shown are the allowed optical transitions (arrows) that lead to excitons X_n ordered by increasing energy.*

Using photoluminescence excitation spectroscopy, Norris and

Bawendi determined the transition energies in CdSe QDs of many different sizes and related them to the transitions in the effective-mass model.[49] The agreement is generally qualitatively good, although the model does not reproduce the size dependence of the energy levels perfectly. It should also be noted that weak, unresolved transitions were treated as a cubic background.

Instead of treating a QD as a large atom, it is possible to treat every atom in the crystal explicitly with quantum chemistry methods. In an atomistic description of QDs, the general pattern of *S* and *P* bands remains but every band consists of many transitions where thousands of electrons can be involved.[50]

3.2 Dynamics of charge carrier relaxation

In solid state physics, the Bohr radius is a measure of the size of a particle in a material. The characteristic optical properties of QDs appear when the QD is comparable in size to the Bohr radius of the exciton inside. The strictest case is the so-called strong confinement regime, where the Bohr radius of the exciton is much larger than the radius of the QD. In this case, the electron and hole will partially cease to behave as an exciton and can act independently of each other.[51] In CdSe QDs, this happens when the QD radius is less than 6 nm.[3] This means that relaxation can be treated as two processes happening in parallel: relaxation of electrons and relaxation of holes.

Relaxation in QDs can happen by several different mechanisms, namely Auger relaxation, surface ligand-induced nonadiabatic relaxation and longitudinal optical phonon emission. The two latter can occur to both electrons and holes, but are faster for holes due to the closer spacing of energy levels in the valence band. Auger relaxation happens essentially only to electrons. The process itself, where the electron transfers its energy to a hole, is in principle reversible, but after it has taken place, the hole relaxes by the other mechanisms back to the band-edge state making the overall process unidirectional. Auger relaxation is the fastest of the three processes for a given energy difference, but is unlikely if the hole is trapped.[52]

3.3 Elucidating charge carrier pathways: Paper I

In Paper **I**, we study the decay pathways of electrons and holes in 3-MPA-capped QDs by 2D electronic spectroscopy. Two examples of 2D spectra are given in Figure 3.2.

The high resolution of 2DES and separation of homogeneous and inhomogeneous broadening is not only useful for dynamics, but also for identifying the excitonic states themselves. After 10 ps population time, all excited QDs will be in the lowest ex-

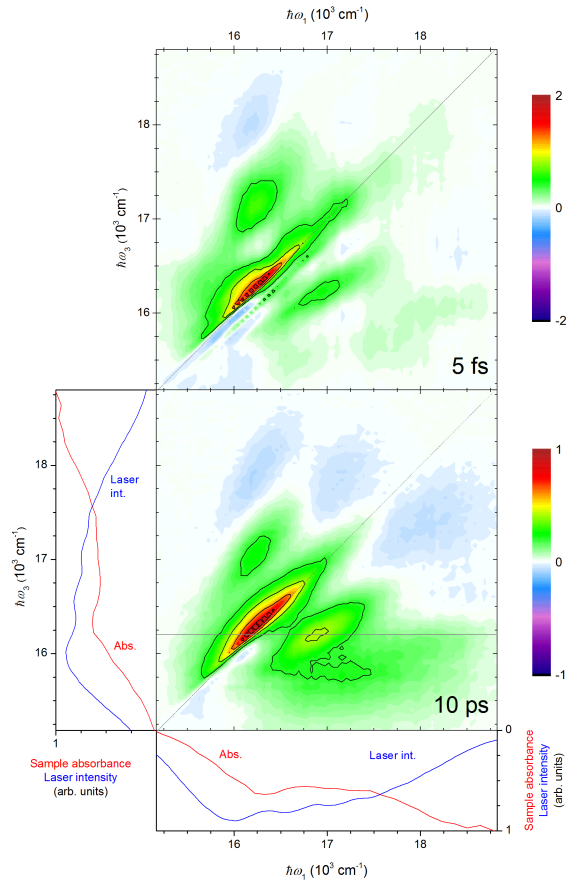

Figure 3.2. *Top panel: Total real 2D spectrum of 7.1 nm CdSe quantum dots in methanol/ethanol glass at 77 K, at 5 fs. The diagonal line marks where $\hbar\omega_1 = \hbar\omega_3$. Middle panel: The same, at 10 ps. The horizontal line marks where a cut was taken for state analysis. Note the rescaling by a factor 2. Side and bottom panels: Sample absorbance (red line) and spectrum of the laser employed in the 2D experiment (blue line) in arbitrary units.*

cited state,[52] and by cutting through the total amplitude 2D spectrum at the $\hbar\omega_3$ of the lowest state (16 200 cm^{-1}), we could identify the energies of all involved states and match them to the effective-mass model as shown in Figure 3.1. The state energies are consistent with the peaks in the absorption spectrum, but fitting from the absorption spectrum alone would lead to larger uncertainty due to inhomogeneous broadening. The lowest spectral band, which is very weak, was assigned to a shallow hole trap combined with the $|1S_e\rangle$ electron state.

When looking at the dynamics, the most common decay

process on these timescales is actually trapping, which we will return to in Chapter 4. However, some relaxation processes are still relevant, and will be discussed here.

The relaxation of the $|1P_{3/2}\rangle$ hole to the $|1S_{3/2}\rangle$ state has not been observed directly, but is expected to be very fast ($\sim$10 fs lifetime) from energy considerations.[52] After exciting into the $|1P_{3/2} - 1P_e\rangle$ ($|X_4\rangle$) state, the QDs should transfer to the $|1S_{3/2} - 1P_e\rangle$ state (which has no strong absorption from the ground state for symmetry reasons) before the hole can be trapped.

When the hole is in the $|1S_{3/2}\rangle$ state, Auger relaxation competes with hole trapping. Hole trapping has a time constant of $\sim$50 fs and Auger relaxation on the order of 100–200 fs,[52] so the majority of holes are trapped but a considerable minority contribute to the Auger pathway.

We also see population transfer from the $|1S_{1/2} - 1S_e\rangle$ to the $|1S_{3/2} - 1S_e\rangle$ state, contradicting the earlier assumption that holes decay sequentially to the next lower-energy state.

To summarize, using 2D electronic spectroscopy, we directly observed state-resolved energy relaxation in thiol-capped functionalized CdSe quantum dots. We exploit the benefits of using very short pulses (FWHM 10 fs) and low-temperature measurements decreasing the overlap between states due to homogeneous broadening. This allows us to track down relaxation pathways, state-by-state, even for times well below 100 fs. We see signals showing relaxation of $|1S_{1/2}\rangle$ holes to $|1S_{3/2}\rangle$ as well as indirect evidence from lifetime considerations of Auger relaxation of $|1P_e\rangle$ electrons to $|1S_e\rangle$. Furthermore, we see a number of trapping processes, which we will return to in Chapter 4 where we complete the picture of photophysical processes within thiol-capped CdSe quantum dots.

Chapter 4

Trapping

Trapping of holes and electrons in quantum dot surface states competes with energy transfer and charge transfer. The trapping is localizing the charges, thus decreasing the probability that the excited electrons and holes will reach the solar cell electrodes. Understanding trapping is therefore important for the design of efficient quantum dot solar cells.

4.1 Theory of trapping

Traps are localized electronic excited states with long lifetimes, so called because they "trap" the charge carrier. They are a feature of QDs that are not present in atoms, but they do not occur in a theoretical perfectly crystalline bulk material either, assuming it is infinite in all directions. They do appear at discontinuities in the crystal structure,[53] which in QDs means the surface (unless all dangling bonds have been passivated by capping agents) but can also be internal defects and ligand states. The presence of traps in QDs is detrimental to QD solar cells, as trapped charge carriers often cannot be harvested[54–57] when trapping competes with relaxation and charge carrier injection.

In QDs, trapping can happen to both holes[58,59] and electrons[60]. Exchanging the capping agent to a thiol such as 2-MPA or 3-MPA creates new traps, mainly hole traps,[61] which is an issue for QDs that should be attached to a surface in solar cells. By studying trapping, we can understand how it limits solar cell efficiency, and what needs to be done to diminish it.

4.2 Detecting trapping: Paper II

In Paper **II**, we identified and characterized deep, long-lived trap states in three sizes of core CdSe QDs with oleic acid as capping agent. In steady-state photoluminescence emission spectra, a

broad feature which can be resolved into two Voigt-profile peaks appears below the band gap energy, indicating that several different surface states exist. In photoluminescence excitation spectra, a band below the band gap fluorescence appears when exciting above the band edge, indicating that trapping takes place mainly from higher-lying states. In time-resolved photoluminescence, the emission below the band gap (selected with a cut-off filter) remains for more than 1 μs (a biexponential decay with lifetimes 63 and 400 ns) where the band-gap emission has disappeared, showing that carriers in these traps cannot become delocalized and return to the band-gap excited state. In transient absorption, a long-lived photobleach (tens of microseconds) attributed to electrons filling the conduction band[61] shows that electrons are not trapped, verifying that the trapped charge carriers are holes.

4.3 Trapping as a limiting factor of solar cells: Paper III

In Paper **III**, we also investigated hole trap states, but this time in a context closer to application in solar cells, namely QDs attached to a hole acceptor. The goal of this project was to extract the hole efficiently, which would form a step in the circuit of a p-type solar cell[62,63]. Hole extraction is limited by competition from trapping, so for this reason, knowledge of the trapping process is needed.

Four different sizes of QDs were studied. In preparation of the attachment, the capping agent was 3-MPA, which introduces traps. The same QDs capped with oleic acid (OA) were used as a reference. Here, we will summarize the characterization of the hole trapping itself, which was done on unattached QDs. In Chapter 5, we will see what happens when hole injection competes with trapping, and how the injection process can be improved.

Analogously to Paper **II**, transient absorption and time-resolved photoluminescence were compared to identify trapping. In OA-capped QDs, the TA signal is almost constant over the short time window (70 ps), but the PL signal decays, showing that hole trapping takes place. Transient absorption is not affected by the change of capping agent, but a new fast component (4 ps lifetime) appears in PL of 3-MPA-capped QDs. This component is diminished after photoirradiation due to the photoinduced emission enhancement effect (PEE), which is caused by surface passivation and photoactivation.[64–68] The slower component is attributed to trapping by intrinsic defects.

4.4 Trapping versus relaxation: return to Paper I

Now, let us take another look at the 2DES results that we started to discuss in Chapter 3.

Following the stimulated emission when holes are excited into the $|1S_{3/2}\rangle$ and $|2S_{3/2}\rangle$ states showed that holes are efficiently trapped directly into a shallow trap state from these states. The electron bleach signal remains, showing that there is no electron trap state accessible from $|1S_e\rangle$. Together with the already mentioned relaxation of $|1S_{1/2}\rangle$ holes to $|1S_{3/2}\rangle$, these pathways are summarized in Figure 4.1.

After excitation into the $|1P_{3/2} - 1P_e\rangle$ state, a strong excited state absorption is growing in, which was assigned to trapping of the electron from the $|1P_e\rangle$ state, competing with Auger relaxation. Auger relaxation is disabled by hole trapping from the $|1S_{3/2}\rangle$ state and possibly also the $|1P_{3/2}\rangle$ state, which means that the majority of electrons will be trapped rather than relaxing to the $|1S_e\rangle$ state. The various pathways from the $|1P_{3/2} - 1P_e\rangle$ state are summarized in Figure 4.2.

Using 2D electronic spectroscopy, we observe direct rapid trapping of $1S_{3/2}$ and $2S_{3/2}$ holes, and $1P_e$ electrons, without proceeding through any lower electronic state of the QD. Thus, we see that the presence of traps entirely changes the relaxation dynamics in the QDs by offering a different efficient channel. Furthermore, we can unambiguously identify the lowest state as a trap, which would not be possible without 2DES.

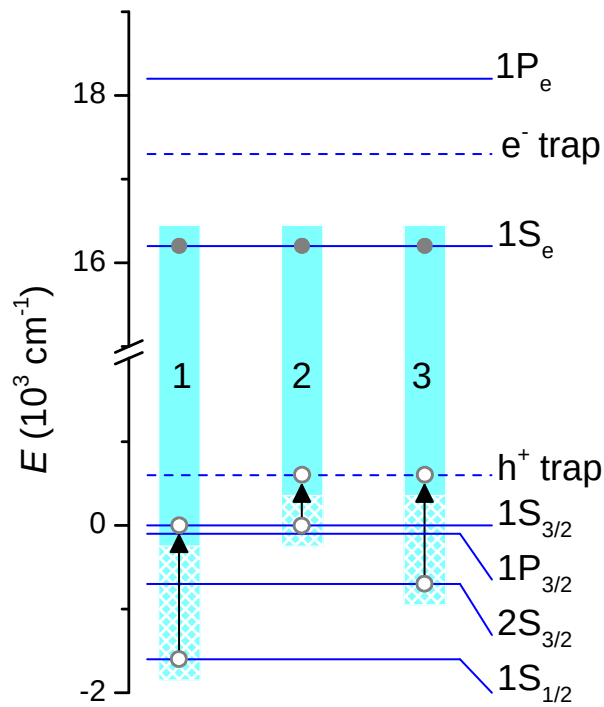

Figure 4.1. *Relaxation and trapping pathways (black arrows) from the three lowest excitonic states in the QDs in Paper* **I**. *Step 1 is followed by step 2 when exciting into* $|X_3\rangle$, *step 2 happens directly after excitation into* $|X_1\rangle$. *Step 3 is the trapping pathway of* $|X_2\rangle$. *The light blue rectangles mark the excitons before (solid and patterned) and after (solid only) each step.*

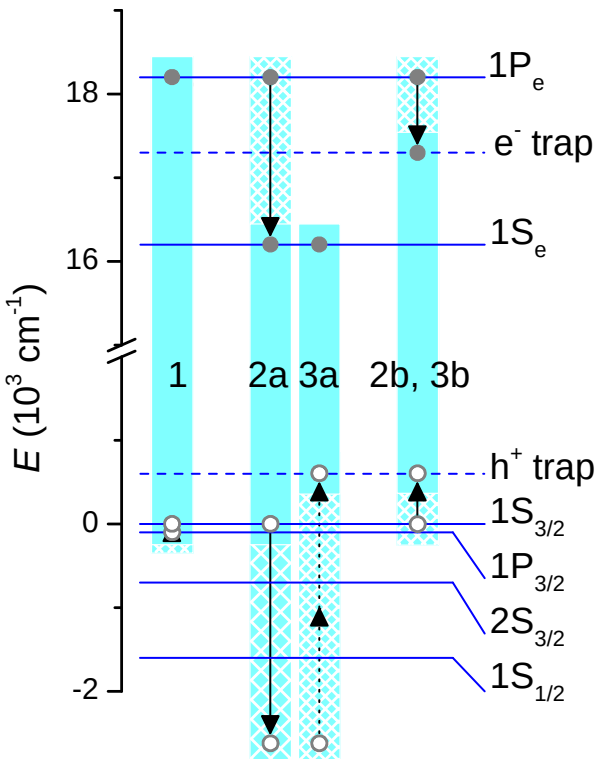

Figure 4.2. *Relaxation and trapping pathways (black arrows) from the $|X_4\rangle$ state in the QDs in Paper* ***I****, assuming the $|1P_{3/2}\rangle$ hole relaxes to $|1S_{3/2}\rangle$ as step 1. Step 2a is Auger relaxation, with the hole going into an unspecified state, and step 3a is the hole relaxation and trapping from this state, which was not studied in detail in our work. Step 2a is prevented by step 2b (electron trapping) or 3a (hole trapping from $|1S_{3/2}\rangle$) which happen in parallel rather than simultaneously. If step 1 does not happen, the rest of the picture will be the same but with the hole in $|1P_{3/2}\rangle$ where it is here in $|1S_{3/2}\rangle$. The light blue rectangles mark the excitons before (solid and densely patterned) and after (solid and sparsely patterned) each step.*

Chapter 5

Energy and charge transfer

In order to create an electric current, the charges generated in a quantum dot must be extracted. Energy transfer can be used to bring the exciton to a place where the charge separation and extraction can take place. The extraction process itself is an example of charge transfer. Quantum dot solar cells can use both electron and hole transfer to achieve the charge separation.

5.1 Energy transfer

Within the context of photochemistry and photophysics, energy transfer is the transfer of excitation energy from one system (molecule, cluster, quantum dot, nanoparticle etc.), the *donor* to another, the *acceptor*. It can take place by a number of mechanisms,[69] of which FRET (fluorescence resonance energy transfer or Förster resonance energy transfer) is the important one in QDs.[70] Depending on the circumstances, it can be described in a number of different ways, but for our purposes, the rate of energy transfer between two point dipoles due to FRET k_{ET} and its corresponding time constant τ_{ET} can be given as[70*]

$$k_{ET} = 1/\tau_{ET} = \left(\frac{2\pi}{\hbar}\mu_D^2\mu_A^2\kappa^2\Theta\right) \Big/ R_{DA}^6 n^4, \tag{5.1}$$

where μ_D and μ_A are the donor and acceptor transition dipoles, κ^2 is the orientation factor of dipole–dipole interaction, Θ is the overlap integral of the normalized donor emission and acceptor absorption spectra, R_{DA} is the distance between donor and acceptor, and n is the refractive index of the medium. There are a number of points to be made here:[70,71]

[*]Compare Equation 2 in Paper **IV**, but note that the right-hand side of the equation was accidentally inverted there.

- The FRET rate is strongly distance-dependent.
- The overlap integral involves the spectra, but no photons are emitted or absorbed during FRET.
- As the spectra of QDs change with size, a set of QDs with different sizes can form a chain with good spectral overlap and thus efficient FRET in each step.
- On the length scale of FRET, QDs are large, and the edge-to-edge QD–QD distances in QD films are small.

We investigated the role of FRET in QD films in Paper **IV** as we will describe in detail later.

5.2 Energy transfer as a harvesting mechanism: Paper IV

As alluded to before, FRET can be a useful tool for solar energy harvesting in QDSSCs. The efficiency-limiting factor of a solar cell based on metal oxide nanoparticles covered by a single layer of QDs is likely absorption rather than injection.[72] By coating a material that accepts either electrons or holes with layers of successively smaller QDs (with increasing band gap), the system can absorb a wide range of wavelengths efficiently and deliver the energy to the QDs closest to the acceptor material by energy transfer, thus increasing efficiency. In Paper **IV**, we measured the FRET dynamics of such films, and analyzed the results in terms of a FRET model that takes the size and packing of QDs into account.

We used three sizes of QDs, labelled A, B, and C in order of increasing size. Solutions and films with one and two QD sizes were prepared, and TA spectra measured for a number of time points up to 10 ns. The TA spectrum of a mixture $\Delta\alpha_{x+y}(t)$ was fitted as the weighted sum of corresponding TA spectra of the components:

$$\Delta\alpha_{x+y}(t) = k_x(t)\Delta\alpha_x(t) + k_y(t)\Delta\alpha_y(t), \tag{5.2}$$

where x is the label of the QDs with larger band gaps, which will be donors if FRET happens, and *vice versa*. The weights will remain constant, i.e. equal to $k_{x,y}(0)$, if there is no FRET. If FRET happens, k_y will increase with time as energy is transferred to the acceptor QDs. The ratio of transferred excitons at time t will be $(k_y(t) - k_y(0))/k_y(0)$ and will increase with time, which is indeed what we see in the films, see Figure 5.1.

The experimental results were compared to a detailed theoretical model. As was mentioned before, the centre-to-centre distance between QDs in the film is significantly larger than

the edge-to-edge distance of the dots, meaning that the point dipole approximation might be too severe. Furthermore, FRET calculations usually assume ideal QD stacking, which is not the case here. To compensate for the size effect, we modelled the QDs as 8000 point dipoles with strengths distributed according to a Bessel function representing the transition densities[73] and calculated the interaction term between the transition densities in different QDs. Then, we simulated random stacking of QDs, and calculated the FRET rate according to the transition density model, yielding a distribution of FRET lifetimes. As we can see in Figure 5.1, the model agrees very well with the data.

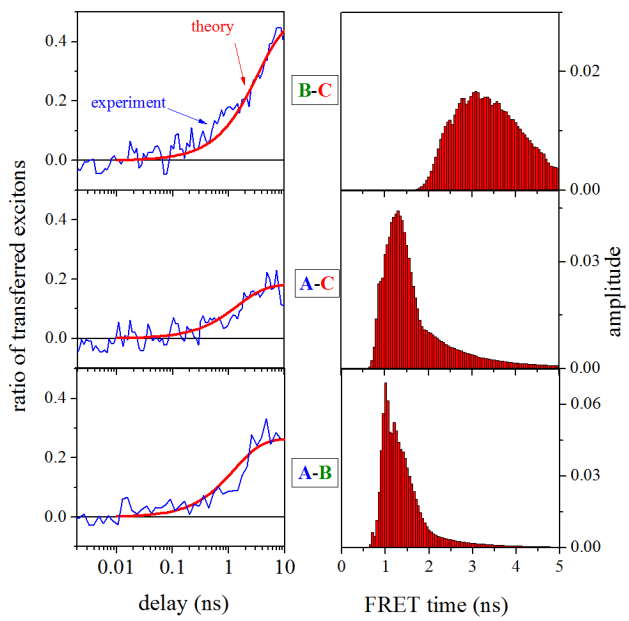

Figure 5.1. *Ratio of transferred excitons and distribution of FRET lifetimes. Left panels: experimental ratio of the excitons transferred (0 means no FRET, 1 means all excitons transferred) to donor (blue lines) compared to the theoretical prediction (red line). Right panels: distribution of FRET lifetimes for each modelled case. Figure courtesy of Karel Žídek.*

For efficient use of energy transfer, directionality in terms of energy levels should be combined with directionality in terms of geometry. The results above were achieved for random QD films, which is suitable for studying the D–A FRET transfer, however, such films cannot provide the desired directed energy transfer. Therefore, measurements and simulations were also made on

films with layers of QDs ordered by size. The ordered layers were achieved via sequential spin-coating, in the order C, B, A or C, B, B, A, see 5.2. Steady-state fluorescence was measured before and after addition of the A layer. The drop in the share R_{AC} of excitons transferred from A to C as the extra B layer ratio is added can be calculated as:

$$\frac{R_{AC}^{A2BC}}{R_{AC}^{ABC}} = \frac{I_C^{A2BC} - I_C^{2BC}}{I_C^{ABC} - I_C^{BC}}, \tag{5.3}$$

where I_C is the integrated fluorescence intensity in the spectral range where C fluoresces. The experimental value was 0.8, and the theoretical 0.75.

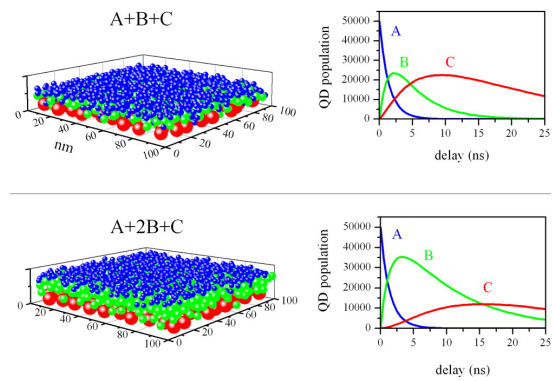

Figure 5.2. *Theoretical simulation of FRET in ordered QD films. Upper panel, left: A QD film consisting of three monolayers of A, B, and C QDs, respectively (blue, green, and red). Right: Calculated population of excited QDs of each size after a random A-type QD is excited. Lower panel: Analogous graphs for a film with two layers of B-type QDs. Figure courtesy of Karel Žídek.*

Furthermore, the effect of increasing numbers of B layers were studied. Here, different numbers of B monolayers were covered by a monolayer of C QDs. By measuring the fluorescence before and after addition of the C layer, the exciton diffusion length can be calculated from the one-dimensional diffusion equation.[74–76] The exciton diffusion length was 9 nm, which shows that efficient energy transfer through more than two layers of QDs of the same size is not possible.

In summary, we have quantified FRET kinetics and yields in random and ordered films by transient absorption and steady-state photoluminescence spectroscopy. Our investigations show

that FRET can be a useful tool in QDSSCs, and that an accurate description of FRET in closely packed QDs requires going beyond the point dipole approximation.

5.3 Charge transfer

In QD solar cells, a crucial step is the extraction of the generated charge from the QD. As we mentioned briefly in Chapter 4, it is most commonly the case that the electron is extracted to the metal oxide as the first step,[77–79] but it is also possible to extract the hole[62,63]. In the first case, the metal oxide is of n-type, in the second case of p-type (see Figure 5.3).

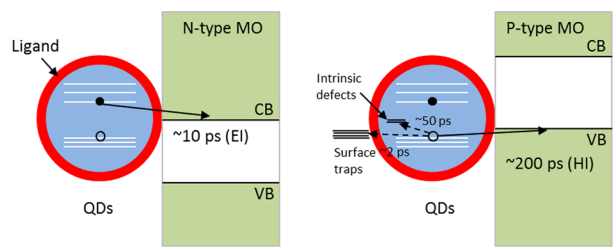

Figure 5.3. *Schematics of electron (left) and hole (right) injection from a QD to a metal oxide. Time scales from*[24] *and*[80]*. Figure courtesy of Kaibo Zheng.*

Charge transfer is often analyzed with Marcus theory, where the donor and acceptor potentials are described as overlapping quadratic curves.[69] In the specific case of injection from a QD with discrete states to a metal oxide with a continuum of states, the expression for the injection rate k_{inj} of the charge carrier becomes[24,81]:

$$k_{inj} = \frac{2\pi |\bar{H}|^2}{\hbar\sqrt{4\pi\lambda k_B T}} \int_{-\infty}^{\infty} \rho(E) \exp\left(-\frac{(\lambda + \Delta G + E)^2}{4\lambda k_B T}\right) \mathrm{d}E, \quad (5.4)$$

where $|\bar{H}|$ is the electronic coupling matrix element (assuming it does not depend strongly on the energy E), λ is the system reorganization energy, k_B is the Boltzmann constant, T is the temperature, $\rho(E)$ the density of unoccupied states in the acceptor, and ΔG is the free energy change of injection. ΔG in turn is the sum of the difference in charge carrier state energy ΔE_{el} or ΔE_{hl} and the difference in Coulomb interaction between the

excited electron and hole ΔE_C. While Marcus theory is usually formulated for electrons, it works equally well for holes.

5.4 Hole transfer versus trapping: Paper III

Let us return to Paper **III** and look at what happens when QDs are attached to a NiO mesoporous film. This is a p-type metal oxide, therefore we expected to see hole injection. This was studied with transient absorption spectroscopy and time-resolved photoluminescence in order to disentangle hole and electron dynamics.

In the TA signal, a new component appeared that is increasing in amplitude with a time constant of roughly 200 ps in 3.0 nm QDs. It is shaped like the first derivative of the absorption spectrum, indicating a shift of the absorption spectrum. A spectral redshift of a few meV is a typical consequence of negative QD charging.[61,82,83]

In the PL, the $\sim$50 ps intrinsic defect trapping component is unaffected, but the component corresponding to the natural lifetime of the excited state is replaced by a faster component (380 ps in 3.0 nm QDs), which within the fitting error is the same time constant as the one in TA assigned to injection. The fast component that disappears with PEE in unattached QDs is unaffected here, suggesting that attachment inhibits or circumvents the PEE process.

The injection time constants are dependent on QD size, consistent with a reorganization energy $\lambda = 190$ meV in the Marcus theory. Furthermore, the relative amplitudes of trapping and injection can be used to calculate an injection efficiency of $\sim$10%, consistent with incident-photon-to-current measurements in real solar cells with CdSe QD-sensitized NiO as photocathodes.[†62]

Thus, we have seen that if hole injection is to be used in efficient solar cells, surface trapping must be reduced. One way of accomplishing this is through employing core–shell structures. In well-designed core–shell QDs, the fast trapping PL component disappears. The hole injection lifetime is increased due to the decreased overlap, yet due to decreased trapping, the injection efficiency increases to 50%.

5.5 Electron transfer versus recombination: Paper V

One of the promising aspects of QDs for solar cells is the possibility of forming multiple electron–hole pairs (excitons) from one absorbed photon, the so-called multiple exciton generation

[†]Paper **III** erroneously uses "incident-current-to-photon" and "photoanode".

or MEG. If MEG is going to be a useful process in solar cells, the multiple excitons must not only be generated, they must also be extracted from the QD before they decay. We will describe the behaviour of multiple excitons in one QD in more detail in Chapter 6, so as for now, let us just consider multiple exciton decay as a process competing with injection. This competition was studied in Paper **V**. QDs attached to ZnO nanoparticles, where electrons can be extracted, were compared to QDs in a film without ZnO. Multiple excitons were created not by MEG as such, but by using high-intensity laser pulses.

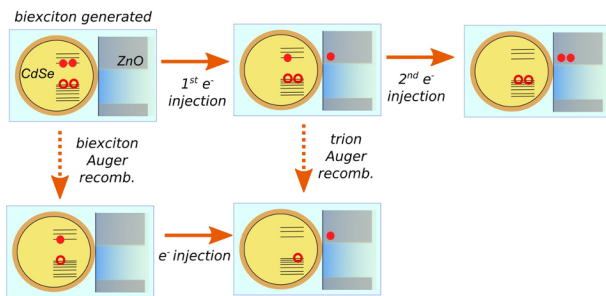

Figure 5.4. *Scheme summarizing the various processes that can lead to electron injection into ZnO from a QD with a biexciton. Figure courtesy of Karel Žídek.*

The various processes that can lead to electron injection into ZnO from a QD with two excitons (a biexciton) are shown in Figure 5.4. We studied these processes in QDs with three shell thicknesses. Electron injection appears as faster TA decay after QDs are attached to ZnO, but the rate decreases with increased shell thickness. Electron injection through a shell is a complex process with a distribution of lifetimes, but it is possible to determine the mean rate by comparing the mean lifetimes of attached and unattached QDs:

$$\langle k_{inj} \rangle = 1/\langle \tau_{\mathrm{QD-ZnO}} \rangle - 1/\langle \tau_{\mathrm{QD}} \rangle. \tag{5.5}$$

This was determined under low-intensity (single-exciton) conditions for the injection itself. When two electron–hole pairs are generated, this is the mean rate for the injection of the first electron. The injection rate for the second electron is expected to be slower as the electron is affected by the charge on the QD and the electron already present in the metal oxide. The lifetime of the trion (the electron–hole–hole combination after one electron has been injected) when Auger recombination and electron injection compete in the core QDs is ∼50 ps, which puts an upper limit on

the rate of the injection (compared to a mean lifetime of 6 ps for injection of the first electron). The actual value is not possible to determine without deeper knowledge of the trion recombination. As we shall see in Chapter 6 when we return to Paper **V**, this information can only be estimated from literature values, where it is not readily available.

Chapter 6

Multiexcitons

One distinct difference between quantum dots and bulk semiconductors is the interaction of excitons. In bulk semiconductors, the exciton density is continuous and on average low compared to a quantum dot with even a single exciton. In quantum dots, on the other hand, exciton density is discrete, giving rise to a number of interesting phenomena.

6.1 Excitons

As we mentioned in Chapter 3, the combination of an electron and a hole can behave as a quasiparticle, called an exciton. More specifically, this happens due to Coulomb interaction. The bound electron–hole pair has lower energy than the individual charge carriers and can transport energy by moving around in the crystal.[48]

Depending on the type of crystal, there are different kinds of excitons. In semiconductors, the excitons are of the Wannier–Mott type, where the electron and hole are weakly bound and quite far from each other (several lattice constants on average) in the bulk.[48] As the effective mass of the hole is much higher than that of the electron, the Wannier–Mott exciton behaves similarly to a hydrogen atom and can even form excitonic molecules, or biexcitons.[84]

6.2 Excitons and multiexcitons in quantum dots

When the crystal size approaches the Bohr radius of the exciton, as is the case in QDs, the behaviour of the exciton is naturally affected. As we remarked in Chapter 3, an electron and a hole act independently of each other under strong confinement conditions (where the Bohr radius of the exciton is smaller than the radius of the QD). The distance between the electron and hole is no

longer determined by the Coulomb interaction, but rather by the size of the crystal. Nevertheless, an electron and hole together are still often described as an exciton.

An important difference between bulk materials and QDs is that while the number of excitons in a given volume of bulk material is continuous, it is discrete in QDs—there cannot be only a third of an exciton in one QD. Instead, there are biexctions, triexcitons, tetraexcitons etc.[85] On the other hand, it is possible to have unequal numbers of electrons and holes if the QD is charged, for example as a trion (one electron, two holes).[84,86]

The discreteness of excitons in QDs means that the kinetics of exciton decay is different from bulk materials. In bulk materials, the density of excitons decreases continuously and nonexponentially after an excitation event. In QDs, it happens stepwise, i.e. one of the electron–hole pairs in a tetraexciton recombines giving a triexciton and so forth. Each such step is exponential with a characteristic lifetime.[85,87]

6.3 Auger recombination

Auger recombination is a process where an excited electron is recombined with a hole and the energy which is released excites another charge carrier. In QDs, this process is more efficient than in bulk semiconductors, due to relaxed demands for momentum conservation. Thus, for example, the recombination of one exciton excites the electron, hole or both in another exciton within a QD.[25,85,86]

The reverse process, where a high-energy exciton forms two lower-energy excitons, is also possible. This is known as impact ionization and is the mechanism behind multiple exciton generation (MEG, also known as carrier multiplication) in QDs.[25,61] In the context of solar cells, MEG is a very attractive phenomenon, as it means that the Shockley–Queisser limit can be avoided by creating several excitons out of a single photon with energy much higher than the band gap.[25–28] After the first report of MEG in 2004,[25] it has been heavily investigated, but contradictory yields have been reported[88–92]. Explanations that have been put forward include surface trapping and charging, which leads to trion formation.[93–95]

6.4 Formation and disappearance of multiexcitons: Paper VI

As mentioned above, there are many confounding effects that must be considered when investigating multiple exciton generation. One such effect is that the amount of multiexcitons formed by impact ionization must be distinguished from the amount

formed by the more pedestrian sequential absorption of photons. Another important parameter is the amount of expected signal (bleach, excited-state absorption and stimulated emission) from the singly and doubly excited QDs. This was studied in Paper **VI** by following the transient absorption kinetics of QDs under different excitation intensities. The series of absorption events leading to a multiexciton is too fast to be resolved in TA, but by analyzing the decay of multiexcitons, the absorption cross sections of each step can be determined.

We tested the method on samples with different sizes, different shell thicknesses and different probe positions relative to the first absorption peak. For each sample, we used four excitation intensities. The lowest intensity I_0 was generally chosen to give almost only singly excited QDs.

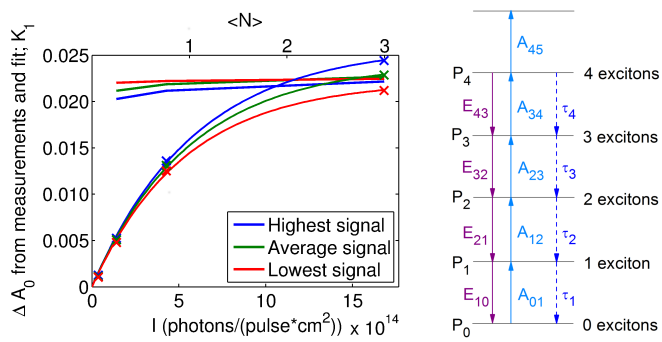

Figure 6.1. *Left: Maximum, average and minimum TA signal (crosses) ΔA_0 rescaled from $t > 6$ ns as a function of excitation intensity (lower axis) and average number of excitons per QDs (upper axis) for sample L0 (core QDs with radius 5 nm) probed at 592 nm, fits according to Eq. 6.1, and K_1, the initial signal if all QDs would contain exactly one exciton (from the three higher-intensity measurements). Right: Kinetic model containing 6 levels describing the multiexciton dynamics and corresponding TA signal. P_N is the population of the N-exciton level, A and E represent absorptive and emittive transition strengths between neighbouring levels, τ_N are the multiexciton Auger recombination times, and τ_1 is the one-exciton decay time.*

The TA kinetics were described by a kinetic model, where the initial population distribution is Poissonian as we pump away from the band edge[85,96,97]. By rescaling the single-exciton signal at long times to $t = 0$, call it ΔA_0, the Poisson distribution gives:

$$\Delta A_0(I) = \Delta A_{0,max} \cdot (1 - e^{-\frac{I}{I_0} \cdot \langle N \rangle_0}), \tag{6.1}$$

where I is intensity and $\langle N \rangle_0$ the average number of excitons per QD at intensity I_0. Thus, we fitted $\langle N \rangle_0$ (see Figure 6.1) and calculated the initial population distribution. The population dynamics were calculated using simple Pauli master equations (see Figure 6.1) and time constants τ_N from fits to the transient absorption traces.

Finally, the TA signal due to the N-exciton population $P_N(t)$ was extracted from

$$S_N(t) = (A_{N,N+1} - E_{N,N-1} - A_{01}) \cdot P_N(t) = K_N \cdot P_N(t), \quad (6.2)$$

where $A_{N,N+1}$ is absorption from the level N to the level $N+1$, $E_{N,N-1}$ is the stimulated emission from level N to $N-1$ and A_{01} is the ground-state bleach.[55] Coefficients K_N defined by the second equation can be seen as the (sample-specific) signal from the level N if all population is on that level, $P_N = 1$. This enables a consistency check: the rescaled long-time signal should approach K_1 at high intensities, and it does (see Figure 6.1).

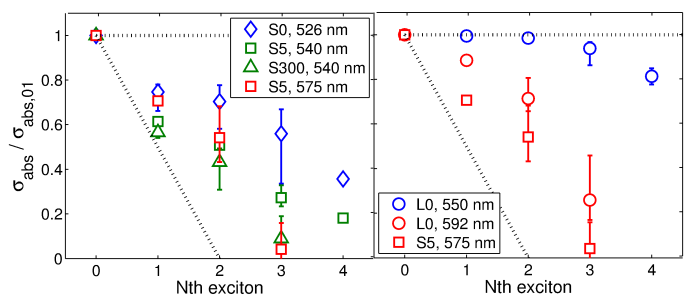

Figure 6.2. *Relative absorption cross sections for the $N \to N+1$-exciton transitions. The error bars were calculated by repeating the fitting procedure with the time constants fixed at their maximum (minimum) values as estimated from a semilogarithmic plot. The dotted lines show the behaviour predicted by the state-filling model and the constant model. All data calculated from the highest pump intensity. Left: The small samples (radius 3 nm). Right: The large sample probed at the band edge (592 nm) and away from the band edge (550 nm) compared with the S5 sample at the band edge.*

Based on Equation 6.2, we get a system of equations that results in the multiexciton absorption cross sections. Results are shown in Figure 6.2. Two limiting cases have been compared with these cross sections: either the cross section is constant, or the cross section drops as the $|1S_e\rangle$ state is filled. The constant cross section model corresponds to the case of an unlimited number of final excited states. The $|1S_e\rangle$ state has a degeneracy of two, so in

the state-filling effective mass model, the cross section should be zero from the second exciton onward. While the cross sections go in the general direction predicted by the state-filling model, the quantitative behaviour is a bit different. The deviation is larger when probing further away from the band edge, which indicates that more states are available here. For large QDs (sample L0, radius 5 nm), the pattern approaches the constant model when probing away from the band edge. There is no shell thickness effect for the small QDs, which indicates that charging is not significant.

To summarize, we have developed a method to obtain multiexciton absorption cross sections in QDs. We apply it to different QDs and obtain different patterns of cross sections—qualitatively in agreement with the state-filling effective mass model, but to get quantitative data, a method such as this one is needed.

6.5 Harvesting of multiexcitons: Paper V revisited

Armed with more detailed knowledge about multiexcitons, let us now return to Paper **V** and look at the multiexciton decay processes in detail (vertical arrows in Figure 5.4). In this chapter, we look at the recombination processes that are possible in this system: biexciton Auger recombination (competing with the first injection) and trion Auger recombination (after one injection, competing with the second).

Again, high-intensity light was used to create biexcitons. The biexciton signal was separated from the single exciton in unattached QDs by the same normalization at long times that was used in Paper **VI**. Its lifetime varies from sample to sample but is in the range of tens of picoseconds. In the core QDs, this is much slower than injection. In the core–shell QDs, injection is slowed down and in the QDs with the thickest shell, biexciton Auger recombination is the faster process of the two. Attaching the QDs to ZnO did not affect the biexciton Auger recombination lifetime.

After one electron is injected, a positive trion is formed, most clearly in the core QDs where the first injection step outcompetes Auger relaxation. As we mentioned already in Chapter 5, it is harder to distinguish injection of the electron in a trion from Auger recombination. Trions have been studied extensively in CdSe QDs,[86,98–100] but their lifetime depends heavily on QD properties. As a rough estimate, *negative* trions have eight times longer lifetimes than biexcitons,[86] so if this holds for the positive trion in our QDs, its lifetime would be $\sim$140 ps, long enough that the second electron can be injected.

We observed that there is an optimal QD size for multiexciton injection, as Auger recombination and electron injection rates

depend on QD size in different ways. When QDs are small enough, Auger recombination becomes very fast, and when QDs are large, injection is hindered by misalignment of electronic states.

To summarize, fast electron injection from QD to ZnO can inhibit the unwanted Auger recombination in doubly excited QDs. Efficient energy harvesting from multiple excitons created by MEG is therefore a feasible scenario. Moreover, MEG harvesting efficiency varies significantly with QD size. Therefore, for full utilization of the MEG effect, a combination of band gap tuning and QD size tuning should be used to maximize the benefits of MEG.

Chapter 7

Conclusion

We conclude the thesis by summarizing the results, and pointing out some directions for future research.

7.1 Summary of results

In this thesis, we have explored several fundamental ultrafast processes in colloidal quantum dots that are important both from a theoretical point of view and for their relevance for solar cell applications.

Using 2D electronic spectroscopy, we have followed how electrons and holes relax through the electronic states that could not be distinguished by previously published measurements, demonstrating the power and relevance of this technique to QDs. Furthermore, we have seen how the relaxation can be intercepted by trapping. With different techniques, we have been able to distinguish between trap states with different characteristics with respect to energy level, lifetime and localization.

We have characterized energy transfer in films of QDs of different sizes, and have shown that a proper quantification of this process requires a detailed description of the film and QD geometry.

We have seen how electron and hole transfer is affected by trapping, by the shell in core–shell structures, and by charging of the QD during injection of several excited electrons. Finally, we have studied the formation and decay of multiple excitons in QDs.

Together, these studies form pieces in a puzzle which hopefully will, when completed, show how QDs can be used in efficient and cheap solar cells. They also show the richness of features arising from quantum confinement.

7.2 Future outlook

Which pieces, then, are missing from the puzzle? We will offer some suggestions without expecting to give a full picture.

When it comes to relaxation, a natural next step is relaxation from higher states. For this, two-colour 2DES,[101] where different spectra are used for the first and second beam pairs, would be useful to see the couplings between high and low-energy exciton states. Understanding the higher exciton states could be especially relevant for hot injection.

Like transient absorption is complemented by time-resolved photoluminescence, 2D electronic spectroscopy can be complemented by coherent two-dimensional fluorescence spectroscopy, where four pulses interact with the sample and the fluorescence is measured.[102] In a QD context, it would be especially interesting to use for traps and other dark states. Other output signals, such as the current generated by a solar cell, can also be used for coherent 2D spectroscopy, as coherent 2D photocurrent spectroscopy.[103]

The study of relaxation with 2DES could also be extended in a systematic way to different capping agents and QD sizes, and more broadly to different QD materials. It might even be possible to engineer traps that improve the transfer of electrons and holes.

A way to make use of hole injection would be tandem cells, where both the electron and the hole are injected. This would require more advanced nanoarchitectures, where also energy transfer could play a role.

An issue of more fundamental than applied interest is oscillations in the 2D signal. These can be studied by Fourier transforming even the population time axis,[104] and would lead to more knowledge about quantum dots as such. Another way of introducing a third spectral dimension is the use of fifth-order signals, which has the potential to yield even more detailed information about couplings between different states.[105,106]

Overall, it seems that the future of quantum dot research is bright, with many interesting problems waiting to be explored.

Abbreviations and symbols

BB	Broadband
BBO	Beta barium borate
CB	Conduction band
CCD	Charge-coupled device
CdO	Cadmium oxide
CdSe	Cadmium selenide
cm^{-1}	Reciprocal centimetre
CO_2	Carbon dioxide
$CuInS_2$	Copper indium sulphide
CZTS	Copper zinc tin sulphide
2DES	Two-dimensional electronic spectroscopy
2DIR	Two-dimensional infrared spectroscopy
DSSC	Dye-sensitized solar cell
E	Energy
e^-	Electron
FRET	Fluorescence (or Förster) resonance energy transfer
fs	Femtosecond
FWHM	Full width at half maximum
GaAs	Gallium arsenide
$\hbar$	Planck's reduced constant
h^+	Hole
I^-	Iodide
I_3^-	Triiodide
kHz	Kilohertz
k_{inj}	Rate constant of injection
λ	Reorganization energy
LO	Local oscillator

MEG	Multiple exciton generation
MHz	Megahertz
mm	Millimetre
2-MPA	2-Mercaptopropionic acid
3-MPA	3-Mercaptopropionic acid
μs	Microsecond
N_2	Nitrogen
NB	Narrow-band
Nd:YAG	Neodymium-doped yttrium aluminium garnet
NiO	Nickel oxide
nm	Nanometre
NMR	Nuclear magnetic resonance
NOPA	Nonlinear optical parametric amplifier
ns	Nanosecond
ω	Angular frequency
OA	Oleic acid
PEE	Photoinduced emission enhancement
PL	Photoluminescence
ps	Picosecond
QD	Quantum dot
QDSSC	Quantum dot-sensitized solar cell
R_n	nth trap state
S	Sulphur
Se	Selenium
Si	Silicon
τ	Lifetime
TA	Transient absorption
TiO_2	Titanium dioxide
UV–vis	Ultraviolet–visible
VB	Valence band
Yb:KGW	Ytterbium-doped potassium gadolinium tungstate
X_n	nth exciton state
ZnO	Zinc oxide
ZnS	Zinc sulphide

References

1. Brus, L. E. A Simple Model for the Ionization Potential, Electron Affinity, and Aqueous Redox Potentials of Small Semiconductor Crystallites. *J. Chem. Phys.* **1983**, *79*, 5566–5571.

2. Ekimov, A.; Efros, A.; Onushchenko, A. Quantum Size Effect in Semiconductor Microcrystals. *Solid State Commun.* **1985**, *56*, 921–924.

3. Norris, D. J. In *Nanocrystal Quantum Dots*, 2nd ed.; Klimov, V. I., Ed.; CRC Press, 2010; Chapter 2, pp 63–96.

4. Hollingsworth, J. A.; Klimov, V. I. In *Nanocrystal Quantum Dots*, 2nd ed.; Klimov, V. I., Ed.; CRC Press, 2010; Chapter 1, pp 1–62.

5. Reed, M. A.; Bate, R. T.; Bradshaw, K.; Duncan, W. M.; Frensley, W. R.; Lee, J. W.; Shih, H. D. Spatial Quantization in GaAs–AlGaAs Multiple Quantum Dots. *J. Vac. Sci. Technol. B* **1986**, *4*, 358–360.

6. Griffiths, D. J. *Introduction to Quantum Mechanics*; Pearson Education, 2005; Chapter 2.2, pp 30–40.

7. Aylward, G.; Findlay, T. *SI Chemical Data*, 5th ed.; Wiley, 2002.

8. Smith, A. M.; Nie, S. Semiconductor Nanocrystals: Structure, Properties, and Band Gap Engineering. *Acc. Chem. Res.* **2010**, *43*, 190–200.

9. Murray, C. B.; Norris, D. J.; Bawendi, M. G. Synthesis and Characterization of Nearly Monodisperse CdE (E = Sulfur, Selenium, Tellurium) Semiconductor Nanocrystallites. *J. Am. Chem. Soc.* **1993**, *115*, 8706–8715.

10. Dabbousi, B. O.; Rodriguez-Viejo, J.; Mikulec, F. V.; Heine, J. R.; Mattoussi, H.; Ober, R.; Jensen, K. F.; Bawendi, M. G. (CdSe)ZnS Core–Shell Quantum Dots: Synthesis and Characterization of a Size Series of Highly Luminescent Nanocrystallites. *J. Phys. Chem. B* **1997**, *101*, 9463–9475.

11. Youn, H. C.; Baral, S.; Fendler, J. H. Dihexadecyl Phosphate, Vesicle-Stabilized and in Situ Generated Mixed Cadmium Sulfide and Zinc Sulfide Semiconductor Particles: Preparation and Utilization for Photosensitized Charge Separation and Hydrogen Generation. *J. Phys. Chem. B* **1988**, *92*, 6320–6327.

12. Bae, W. K.; Char, K.; Hur, H.; Lee, S. Single-Step Synthesis of Quantum Dots with Chemical Composition Gradients. *Chem. Mater.* **2008**, *20*, 531–539.

13. Reiss, P.; Protière, M.; Li, L. Core/Shell Semiconductor Nanocrystals. *Small* **2009**, *5*, 154–168.

14. Nawrot, T.; Plusquin, M.; Hogervorst, J.; Roels, H. A.; Celis, H.; Thijs, L.; Vangronsveld, J.; Van Hecke, E.; Staessen, J. A. Environmental Exposure to Cadmium and Risk of Cancer: A Prospective Population-Based Study. *Lancet Oncol.* **2006**, *7*, 119–126.

15. Mattoussi, H. In *Nanocrystal Quantum Dots*, 2nd ed.; Klimov, V. I., Ed.; CRC Press, 2010; Chapter 10, pp 369–396.

16. Pan, Z.; Mora-Seró, I.; Shen, Q.; Zhang, H.; Li, Y.; Zhao, K.; Wang, J.; Zhong, X.; Bisquert, J. High-Efficiency "Green" Quantum Dot Solar Cells. *Journal of the American Chemical Society* **2014**, *136*, 9203–9210.

17. Mitzi, D. B.; Gunawan, O.; Todorov, T. K.; Wang, K.; Guha, S. The Path Towards a High-Performance Solution-Processed Kesterite Solar Cell. *Sol. Energ. Mat. Sol. Cells* **2011**, *95*, 1421–1436.

18. Khare, A.; Wills, A. W.; Ammerman, L. M.; Norris, D. J.; ; Aydil, E. S. Size Control and Quantum Confinement in Cu_2ZnSnS_4 Nanocrystals. *Chem. Commun.* **2011**, *47*, 11721–11723.

19. Grätzel, M. Photoelectrochemical Cells. *Nature* **2001**, *414*, 338–344.

20. O'Regan, B.; Grätzel, M. A Low-Cost, High-Efficiency Solar Cell Based on Dye-Sensitized Colloidal TiO_2 Films. *Nature* **1991**, *353*, 737–740.

21. Kamat, P. V. Quantum Dot Solar Cells. *The Next Big Thing* in Photovoltaics. *J. Phys. Chem. Lett.* **2013**, *4*, 908–918.

22. National Center for Photovoltaics, Best Research-Cell Efficiencies. 2015; http://www.nrel.gov/ncpv/images/efficiency_chart.jpg.

23. Kongkanand, A.; Tvrdy, K.; Takechi, K.; Kuno, M.; Kamat, P. V. Quantum Dot Solar Cells. Tuning Photoresponse through Size and Shape Control of CdSe–TiO_2 Architecture. *J. Am. Chem. Soc.* **2008**, *130*, 4007–4015.

24. Žídek, K.; Zheng, K.; Ponseca Jr, C. S.; Messing, M. E.; Wallenberg, L. R.; Chábera, P.; Abdellah, M.; Sundström, V.; Pullerits, T. Electron Transfer in Quantum-Dot-Sensitized ZnO Nanowires: Ultrafast Time-Resolved Absorption and Terahertz Study. *J. Am. Chem. Soc.* **2012**, *134*, 12110–12117.

25. Schaller, R. D.; Klimov, V. I. High Efficiency Carrier Multiplication in PbSe Nanocrystals: Implications for Solar Energy Conversion. *Phys. Rev. Lett.* **2004**, *92*, 186601.

26. Ellingson, R. J.; Beard, M. C.; Johnson, J. C.; Yu, P.; Micic, O. I.; Nozik, A. J.; Shabaev, A.; Efros, A. L. Highly Efficient Multiple Exciton Generation in Colloidal PbSe and PbS Quantum Dots. *Nano Lett.* **2005**, *5*, 865–871.

27. Trinh, M. T.; Polak, L.; Schins, J. M.; Houtepen, A. J.; Vaxenburg, R.; Maikov, G. I.; Grinbom, G.; Midgett, A. G.; Luther, J. M.; Beard, M. C.; Nozik, A. J.; Bonn, M.; Lifshitz, E.; Siebbeles, L. D. A. Anomalous Independence of Multiple Exciton Generation on Different Group IV–VI Quantum Dot Architectures. *Nano Lett.* **2011**, *11*, 1623–1629.

28. Karki, K. J.; Ma, F.; Zheng, K.; Zidek, K.; Mousa, A.; Abdellah, M. A.; Messing, M.; Wallenberg, L. R.; Yartsev, A.; Pullerits, T. Multiple Exciton Generation in Nano-Crystals Revisited: Consistent Calculation of the Yield Based on Pump-Probe Spectroscopy. *Sci. Rep.* **2013**, *3*, 2287.

29. Žídek, K.; Zheng, K.; Abdellah, M.; Lenngren, N.; Chábera, P.; Pullerits, T. Ultrafast Dynamics of Multiple Exciton Harvesting in the CdSe–ZnO System: Electron Injection versus Auger Recombination. *Nano Lett.* **2012**, *12*, 6393–6399.

30. Ip, A. H. et al. Hybrid Passivated Colloidal Quantum Dot Solids. *Nat. Nanotechnol.* **2012**, *7*, 577–582.

31. Shockley, W.; Queisser, H. Detailed Balance Limit of Efficiency of *p–n* Junction Solar Cells. *J. Appl. Phys.* **1961**, *32*, 510–519.

32. Hanna, M. C.; Beard, M. C.; Nozik, A. J. Effect of Solar Concentration on the Thermodynamic Power Conversion Efficiency of Quantum-Dot Solar Cells Exhibiting Multiple Exciton Generation. *J. Phys. Chem. Lett.* **2012**, *3*, 2857–2862.

33. Giebink, N. C.; Wiederrecht, G. P.; Wasielewski, M. R.; Forrest, S. R. Thermodynamic Efficiency Limit of Excitonic Solar Cells. *Phys. Rev. B* **2011**, *83*, 195326.

34. Bullen, C. R.; Mulvaney, P. Nucleation and Growth Kinetics of CdSe Nanocrystals in Octadecene. *Nano Lett.* **2004**, *4*, 2303–2307.

35. Abdellah, M.; Žídek, K.; Zheng, K.; Chábera, P.; Messing, M. E.; Pullerits, T. Balancing Electron Transfer and Surface Passivation in Gradient CdSe/ZnS Core–Shell Quantum Dots Attached to ZnO. *J. Phys. Chem. Lett.* **2013**, *4*, 1760–1765.

36. Bae, W. K.; Kwak, J.; Park, J. W.; Char, K.; Lee, C.; Lee, S. Highly Efficient Green-Light-Emitting Diodes Based on CdSe@ZnS Quantum Dots with a Chemical-Composition Gradient. *Adv. Mater.* **2009**, *21*, 1690–1694.

37. Yu, W.; Qu, L.; Guo, W.; Peng, X. Experimental Determination of the Extinction Coefficient of CdTe, CdSe, and CdS Nanocrystals. *Chem. Mater.* **2003**, *15*, 2854–2860.

38. Žídek, K.; Zheng, K.; Chábera, P.; Abdellah, M.; Pullerits, T. Quantum Dot Photodegradation Due to CdSe-ZnO Charge Transfer: Transient Absorption Study. *Appl. Phys. Lett.* **2012**, *100*, 243111.

39. Hamm, P.; Zanni, M. *Concepts and Methods of 2D Infrared Spectroscopy*; Cambridge University Press, 2011.

40. Turner, D. B.; Hassan, Y.; Scholes, G. D. Exciton Superposition States in CdSe Nanocrystals Measured Using Broadband Two-Dimensional Electronic Spectroscopy. *Nano Lett.* **2012**, *12*, 880–886.

41. Caram, J. R.; Zheng, H.; Dahlberg, P. D.; Rolczynski, B. S.; Griffin, G. B.; Dolzhnikov, D. S.; Talapin, D. V.; Engel, G. S. Exploring Size and State Dynamics in CdSe Quantum Dots Using Two-Dimensional Electronic Spectroscopy. *J. Chem. Phys.* **2014**, *140*, 084701.

42. Aue, W. P.; Bartholdi, E.; Ernst, R. R. Two-Dimensional Spectroscopy. Application to Nuclear Magnetic Resonance. *J. Chem. Phys.* **1976**, *64*, 2229–2246.

43. Tanimura, Y.; Mukamel, S. Two-Dimensional Femtosecond Vibrational Spectroscopy of Liquids. *J. Chem. Phys.* **1993**, *99*, 9496–9511.

44. Mukamel, S. *Principles of Nonlinear Optical Spectroscopy*; Oxford University Press, 1995.

45. Hybl, J. D.; Albrecht, A. W.; Gallagher Faeder, S. M.; Jonas, D. M. Two-Dimensional Electronic Spectroscopy. *Chem. Phys. Lett.* **1998**, *297*, 307–313.

46. Augulis, R.; Zigmantas, D. Two-Dimensional Electronic Spectroscopy with Double Modulation Lock-In Detection: Enhancement of Sensitivity and Noise Resistance. *Opt. Express* **2011**, *19*, 13126–13133.

47. Rowland, C. E.; Schaller, R. D. Exciton Fate in Semiconductor Nanocrystals at Elevated Temperatures: Hole Trapping Outcompetes Exciton Deactivation. *J. Phys. Chem. C* **2013**, *117*, 17337–17343.

48. Kittel, C. *Introduction to Solid State Physics*, 8th ed.; Wiley, 2005.

49. Norris, D.; Bawendi, M. Measurement and Assignment of the Size-Dependent Optical Spectrum in CdSe Quantum Dots. *Phys. Rev. B* **1996**, *53*, 16338–16346.

50. Prezhdo, O. V. Multiple Excitons and the Electron–Phonon Bottleneck in Semiconductor Quantum Dots: An *ab Initio* Perspective. *Chem. Phys. Lett.* **2008**, *460*, 1–9.

51. Gaponenko, S. V. *Optical Properties of Semiconductor Nanocrystals*; Cambridge University Press, 1998; Chapter 23.

52. Cooney, R. R.; Sewall, S. L.; Dias, E. A.; Sagar, D. M.; Anderson, K. E. H.; Kambhampati, P. Unified Picture of Electron and Hole Relaxation Pathways in Semiconductor Quantum Dots. *Phys. Rev. B* **2007**, *75*, 245311.

53. Lüth, H. *Solid Surfaces, Interfaces and Thin Films*, 4th ed.; Springer, 2001.

54. Gómez-Campos, F. M.; Califano, M. Hole Surface Trapping in CdSe Nanocrystals: Dynamics, Rate Fluctuations, and Implications for Blinking. *Nano Lett.* **2012**, *12*, 4508–4517.

55. Kambhampati, P. Hot Exciton Relaxation Dynamics in Semiconductor Quantum Dots: Radiationless Transitions on the Nanoscale. *J. Phys. Chem. C* **2011**, *115*, 22089–22109.

56. Hines, M. A.; ; Guyot-Sionnest, P. Synthesis and Characterization of Strongly Luminescing ZnS-Capped CdSe Nanocrystals. *J. Phys. Chem.* **1996**, *100*, 468–471.

57. Kramer, I. J.; Sargent, E. H. Colloidal Quantum Dot Photovoltaics: A Path Forward. *ACS Nano* **2011**, *5*, 8506–8514.

58. Jones, M.; Lo, S. S.; Scholes, G. D. Quantitative Modeling of the Role of Surface Traps in CdSe/CdS/ZnS Nanocrystal Photoluminescence Decay Dynamics. *Proc. Natl. Acad. Sci. U.S.A.* **2009**, *106*, 3011–3016.

59. Kaniyankandy, S.; Rawalekar, S.; Verma, S.; Palit, D. K.; Ghosh, H. N. Charge Carrier Dynamics in Thiol Capped CdTe Quantum Dots. *Phys. Chem. Chem. Phys.* **2010**, *12*, 4210–4216.

60. Omogo, B.; Aldana, J. F.; Heyes, C. D. Radiative and Nonradiative Lifetime Engineering of Quantum Dots in Multiple Solvents by Surface Atom Stoichiometry and Ligands. *J. Phys. Chem. C* **2013**, *117*, 2317–2327.

61. Klimov, V. I. Spectral and Dynamical Properties of Multiexcitons in Semiconductor Nanocrystals. *Annu. Rev. Phys. Chem.* **2007**, *58*, 635–673.

62. Barceló, I.; Guillén, E.; Lana-Villarreal, T.; Gómez, R. Preparation and Characterization of Nickel Oxide Photocathodes Sensitized with Colloidal Cadmium Selenide Quantum Dots. *J. Phys. Chem. C* **2013**, *117*, 22509–22517.

63. Wang, Z.; Shakya, A.; Gu, J.; Lian, S.; Maldonado, S. Sensitization of p-GaP with CdSe Quantum Dots: Light-Stimulated Hole Injection. *J. Am. Chem. Soc.* **2013**, *135*, 9275–9278, PMID: 23745827.

64. Jones, M.; Nedeljkovic, J.; Ellingson, R. J.; Nozik, A. J.; Rumbles, G. Photoenhancement of Luminescence in Colloidal CdSe Quantum Dot Solutions. *J. Phys. Chem. B* **2003**, *107*, 11346–11352.

65. Javier, A.; Strouse, G. F. Activated and Intermittent Photoluminescence in Thin CdSe Quantum Dot Films. *Chem. Phys. Lett.* **2004**, *391*, 60–63.

66. Christova, C. G.; Stouwdam, J. W.; Eijkemans, T. J.; Silov, A. Y.; van der Heijden, R. W.; Kemerink, M.; Janssen, R. A. J.; Salemink, H. W. M. Photoluminescence Enhancement in Thin Films of PbSe Nanocrystals. *Appl. Phys. Lett.* **2008**, *93*, 121906.

67. Nazzal, A. Y.; Qu, L.; Peng, X.; Xiao, M. Photoactivated CdSe Nanocrystals as Nanosensors for Gases. *Nano Lett.* **2003**, *3*, 819–822.

68. Peterson, J. J.; Krauss, T. D. Photobrightening and Photodarkening in PbS Quantum Dots. *Phys. Chem. Chem. Phys.* **2006**, *8*, 3851–3856.

69. Turro, N. J.; Ramamurthy, V.; Scaiano, J. *Principles of Molecular Photochemistry: An Introduction*; University Science Books, 2009.

70. Crooker, S. A.; Hollingsworth, J. A.; Tretiak, S.; Klimov, V. I. Spectrally Resolved Dynamics of Energy Transfer in Quantum-Dot Assemblies: Towards Engineered Energy Flows in Artificial Materials. *Phys. Rev. Lett.* **2002**, *89*, 186802.

71. Lakowicz, J. R. *Principles of Fluorescence Spectroscopy*, 2nd ed.; Kluwer Academic / Plenum Publishers, 1999.

72. Hodes, G. Comparison of Dye- and Semiconductor-Sensitized Porous Nanocrystalline Liquid Junction Solar Cells. *J. Phys. Chem. C* **2008**, *112*, 17778–17787.

73. Krueger, B. P.; Scholes, G. D.; Fleming, G. R. Calculation of Couplings and Energy-Transfer Pathways between the Pigments of LH2 by the ab Initio Transition Density Cube Method. *J. Phys. Chem. B* **1998**, *102*, 5378–5386.

74. Mei, J.; Bradley, M. S.; Bulović, V. Photoluminescence Quenching of Tris-(8-Hydroxyquinoline) Aluminum Thin Films at Interfaces with Metal Oxide Films of Different Conductivities. *Phys. Rev. B* **2009**, *79*, 235205.

75. Menke, S. M.; Luhman, W. A.; Holmes, R. J. Tailored Exciton Diffusion in Organic Photovoltaic Cells for Enhanced Power Conversion Efficiency. *Nat. Mater.* **2013**, *12*, 152–157.

76. Scully, S. R.; McGehee, M. D. Effects of Optical Interference and Energy Transfer on Exciton Diffusion Length Measurements in Organic Semiconductors. *Journal of Applied Physics* **2006**, *100*, 034907.

77. Santra, P. K.; Kamat, P. V. Mn-Doped Quantum Dot Sensitized Solar Cells: A Strategy to Boost Efficiency over 5%. *J. Am. Chem. Soc.* **2012**, *134*, 2508–2511.

78. Leschkies, K. S.; Divakar, R.; Basu, J.; Enache-Pommer, E.; Boercker, J. E.; Carter, C. B.; Kortshagen, U. R.; Norris, D. J.; ; Aydil, E. S. Photosensitization of ZnO Nanowires with CdSe Quantum Dots for Photovoltaic Devices. *Nano Lett.* **2007**, *7*, 1793–1798.

79. Jovanovski, V.; González-Pedro, V.; Giménez, S.; Azaceta, E.; nero, G. C.; Grande, H.; Tena-Zaera, R.; Mora-Seró, I.; Bisquert, J. A Sulfide/Polysulfide-Based Ionic Liquid Electrolyte for Quantum Dot-Sensitized Solar Cells. *J. Am. Chem. Soc.* **2011**, *133*, 20156–20159.

80. Zheng, K.; Žídek, K.; Abdellah, M.; Zhang, W.; Chábera, P.; Lenngren, N.; Yartsev, A.; Pullerits, T. Ultrafast Charge Transfer from CdSe Quantum Dots to p-Type NiO: Hole Injection vs Hole Trapping. *J. Phys. Chem. C* **2014**, *118*, 18462–18471.

81. Tvrdy, K.; Frantsuzov, P. A.; Kamat, P. V. Photoinduced Electron Transfer from Semiconductor Quantum Dots to Metal Oxide Nanoparticles. *Proc. Natl. Acad. Sci. U.S.A.* **2011**, *108*, 29–34.

82. Stinaff, E. A.; Scheibner, M.; Bracker, A. S.; Ponomarev, I. V.; Korenev, V. L.; Ware, M. E.; Doty, M. F.; Reinecke, T. L.; Gammon, D. Optical Signatures of Coupled Quantum Dots. *Science* **2006**, *311*, 636–639.

83. Hartmann, A.; Ducommun, Y.; Kapon, E.; Hohenester, U.; Molinari, E. Few-Particle Effects in Semiconductor Quantum Dots: Observation of Multicharged Excitons. *Phys. Rev. Lett.* **2000**, *84*, 5648–5651.

84. Pelant, I.; Valenta, J. *Luminescence Spectroscopy of Semiconductors*; Oxford University Press, 2012.

85. Klimov, V. I.; Mikhailovsky, A. A.; McBranch, D. W.; Leatherdale, C. A.; Bawendi, M. G. Quantization of Multiparticle Auger Rates in Semiconductor Quantum Dots. *Science* **2000**, *287*, 1011–1013.

86. Jha, P. P.; Guyot-Sionnest, P. Trion Decay in Colloidal Quantum Dots. *ACS Nano* **2009**, *3*, 1011–1015.

87. Klimov, V. I.; Mikhailovsky, A. A.; Xu, S.; Malko, A.; Hollingsworth, J. A.; Leatherdale, C. A.; Eisler, H. J.; Bawendi, M. G. Optical Gain and Stimulated Emission in Nanocrystal Quantum Dots. *Science* **2000**, *290*, 314–317.

88. Nair, G.; Bawendi, M. G. Carrier Multiplication Yields of CdSe and CdTe Nanocrystals by Transient Photoluminescence Spectroscopy. *Phys. Rev. B* **2007**, *76*, 081304.

89. Nair, G.; Geyer, S.; Chang, L.-Y.; Bawendi, M. Carrier Multiplication Yields in PbS and PbSe Nanocrystals Measured by Transient Photoluminescence. *Phys. Rev. B* **2008**, *78*, 1–10.

90. Trinh, M. T.; Houtepen, A. J.; Schins, J. M.; Hanrath, T.; Piris, J.; Knulst, W.; Goossens, A. P. L. M.; Siebbeles, L. D. A. In Spite of Recent Doubts Carrier Multiplication Does Occur in PbSe Nanocrystals. *Nano Lett.* **2008**, *8*, 1713–1718.

91. Pijpers, J. J. H.; Ulbricht, R.; Tielrooij, K. J.; Osherov, A.; Golan, Y.; Delerue, C.; Allan, G.; Bonn, M. Assessment of Carrier-Multiplication Efficiency in Bulk PbSe and PbS. *Nat. Phys.* **2009**, *5*, 811–814.

92. Nair, G.; Chang, L.-Y.; Geyer, S. M.; Bawendi, M. G. Perspective on the Prospects of a Carrier Multiplication Nanocrystal Solar Cell. *Nano Lett.* **2011**, *11*, 2145–2151.

93. Galland, C.; Ghosh, Y.; Steinbrück, A.; Sykora, M.; Hollingsworth, J. A.; Klimov, V. I.; Htoon, H. Two Types of Luminescence Blinking Revealed by Spectroelectrochemistry of Single Quantum Dots. *Nature* **2011**, *479*, 203–207.

94. McGuire, J. A.; Joo, J.; Pietryga, J. M.; Schaller, R. D.; Klimov, V. I. New Aspects of Carrier Multiplication in Semiconductor Nanocrystals. *Acc. Chem. Res.* **2008**, *41*, 1810–1819.

95. Tyagi, P.; Kambhampati, P. False Multiple Exciton Recombination and Multiple Exciton Generation Signals in Semiconductor Quantum Dots Arise from Surface Charge Trapping. *J. Chem. Phys.* **2011**, *134*, 094706.

96. Ji, M.; Park, S.; Connor, S. T.; Mokari, T.; Cui, Y.; Gaffney, K. J. Efficient Multiple Exciton Generation Observed in Colloidal PbSe Quantum Dots with Temporally and Spectrally Resolved Intraband Excitation. *Nano Lett.* **2009**, *9*, 1217–1222.

97. Cho, B.; Peters, W. K.; Tiwari, V.; Spencer, A. P.; Baranov, D.; Hill, R. J.; Jonas, D. M. Absolute Femtosecond Measurements of Auger Recombination Dynamics in Lead Sulfide Quantum Dots. *EPJ Web of Conferences* **2013**, *41*, 04035.

98. Wang, X.; Ren, X.; Kahen, K.; Hahn, M. A.; Rajeswaran, M.; Maccagnano-Zacher, S.; Silcox, J.; Cragg, G. E.; Efros, A. L.; Krauss, T. D. Non-Blinking Semiconductor Nanocrystals. *Nature* **2009**, *459*, 686–689.

99. Louyer, Y.; Biadala, L.; Tamarat, P.; Lounis, B. Spectroscopy of Neutral and Charged Exciton States in Single CdSe/ZnS Nanocrystals. *Appl. Phys. Lett.* **2010**, *96*, 203111.

100. Marceddu, M.; Saba, M.; Quochi, F.; Lai, A.; Huang, J.; Talapin, D. V.; Mura, A.; Bongiovanni, G. Charged Excitons, Auger Recombination and Optical Gain in CdSe/CdS Nanocrystals. *Nanotechnology* **2012**, *23*, 015201.

101. Myers, J. A.; Lewis, K. L.; Tekavec, P. F.; Ogilvie, J. P. Two-Color Two-Dimensional Fourier Transform Electronic Spectroscopy with a Pulse-Shaper. *Opt. Express* **2008**, *16*, 17420–17428.

102. Tekavec, P. F.; Lott, G. A.; Marcus, A. H. Fluorescence-Detected Two-Dimensional Electronic Coherence Spectroscopy by Acousto-Optic Phase Modulation. *J. Chem. Phys.* **2007**, *127*, 214307.

103. Karki, K. J.; Widom, J. R.; Seibt, J.; Moody, I.; Lonergan, M. C.; Pullerits, T.; Marcus, A. H. Coherent Two-Dimensional Photocurrent Spectroscopy in a PbS Quantum Dot Photocell. *Nat. Commun.* **2014**, *5*, 5869.

104. Seibt, J.; Hansen, T.; Pullerits, T. 3D Spectroscopy of Vibrational Coherences in Quantum Dots: Theory. *J. Phys. Chem. B* **2013**, *117*, 11124–11133.

105. Hamm, P. Three-Dimensional-IR Spectroscopy: Beyond the Two-Point Frequency Fluctuation Correlation Function. *J. Chem. Phys.* **2006**, *124*, 124506.

106. Fidler, A. F.; Harel, E.; Engel, G. S. Dissecting Hidden Couplings Using Fifth-Order Three-Dimensional Electronic Spectroscopy. *J. Phys. Chem. Lett.* **2010**, *1*, 2876–2880.

Acknowledgements

This thesis would not have been possible without the direct involvement of a large number of other people.

Tõnu, your unwavering optimism and openness to discussion really are what carried this project. Many times, I have learnt things from you without even noticing until afterwards, like how to apply for money.

Donatas, you have always been very helpful in all matters 2D, often providing some important perspective like the usefulness of working in liquid nitrogen.

Karel, you only formally became my co-supervisor after a year, but in practice you were from the start. All the late nights and weekends in the laser lab would not have been as easy to survive without our discussions of such things as Czech ABBA covers.

All the coauthors, especially *Mohamed*, *Kaibo*, *Khadga*, *Pavel* and *Tommy*, thank you for all the work we did together, all the discussions and all the fun we had. This also goes out to the rest of the *Pullerits group*, where the strong collaboration and team spirit has not (yet?) resulted in coauthorship.

Mum and *Dad*, you supported me through all this time, and asked all the questions that eventually made writing the popular science summary very easy.

The look of the thesis owes much to my brother *Olle*, who turned my cover idea into something worth putting on the cover, *Jens*, who wrote the LaTeX template and advised me on layout, and the creators of some of the figures, indicated in the captions.

No human being is an island, and there are many people who contributed to the social environment that helped create this thesis, even if it is not possible to pinpoint any specific details in it.

My officemates, especially *Sesha*, *Cornelia* and *Chandramouli*, having you around has been a relief and an opportunity to talk about things not always connected to science. I have learnt a lot about India and a bit about Germany from you, and you have given me reason to examine my own society as well.

Chemical Physics, whether you are a department, a division or something else, you made me feel part of something bigger. I won't try to list everyone who has come and gone during these years for fear of forgetting someone, but thank you all for the seminars, the courses, the chats in the corridor, the lunch room, the trips and the collaborations with other parts of the Chemistry Centre, the Lund Laser Centre and NanoLund. It wouldn't happen without administration, *Maria*, *Thomas*, *Anki* and *Katarina*. I wonder if we will ever find that delivery of milk...

My fellow lab teachers, *Sanna*, *Björn*, *Fredrik*, *Martin* and especially *Tomas*, without whom I would not have ended up in Lund, you made the hard work of grading lab reports fun. *Anita*, your work running all the practical things in the course labs is invaluable. *Students*, you make me learn stuff as well. *Isa*, *Karin* and *Aboma*, I had no idea serving pea soup and pancakes could be so fun.

Svante, you have been my brother-in-arms in both student life and teaching, and brought me to the people at *Thursday evenings at Theoretical Chemistry* and the other inhabitants of the apartment at Magistratsvägen 55P: *Alice*, *Evelina* and *Paulius*. You have all been very important for making me feel at home in Lund.

All my friends from *Uppsala*, *Bergslagen* and further afield, who helped me with my "homesickness" and offered your guest beds when I came to visit (too many to list here!). A special thanks to those who visited me in Lund during this time: *Alve*, *Andreas*, *Jakob*, *Jojo*, *Jonas* and *Petter*. And even though I moved away from many friends, there are also those I moved to: *Andreas*, *Oskar*, *Julia*, *Kalle*, *Martin*, *Sophia*, *Per-Olof*, the *Tuvegårds*, the *Roséns* and the *Hall–Johanssons*, thank you for welcoming me to your city.